

A Four-quadrant Mobility Model-based Routing Protocol for Post-earthquake Emergency Communication Network

Xiaoming Wang

Shanghai Earthquake Administration <https://orcid.org/0000-0002-8328-3805>

Chang Guo (✉ guochang@mail.dhu.edu.cn)

Ping Li

Shanghai Earthquake Agency

Research

Keywords: ECN, FQMM, FQMMP, Rescue Urgency Degree, post-earthquake

Posted Date: July 7th, 2020

DOI: <https://doi.org/10.21203/rs.3.rs-38959/v1>

License: © ⓘ This work is licensed under a Creative Commons Attribution 4.0 International License.

[Read Full License](#)

A four-quadrant mobility model-based routing protocol for post-earthquake emergency communication network

Xiaoming Wang¹, Chang Guo^{2,*}, Ping Li¹

¹ Shanghai Earthquake Administration; wangyoucao78@163.com

² The College of Information, Mechanical, and Electrical Engineering, Shanghai Normal University; guochang@mail.dhu.edu.cn

* Correspondence: guochang@mail.dhu.edu.cn

Abstract: Emergency communication network (ECN) is essential for both disaster victims and rescuers since the pre-deployed network infrastructure may be completely destroyed after the earthquake. Traditional protocols cannot satisfy the requirements of ECN as they neither consider mobility model nor seismic intensity. In this paper, a four-quadrant mobility model (FQMM) based on seismic intensity is proposed for rescuers. Then a FQMM-based protocol (FQMMP) for ECN is designed, which aims to improve the performance of ECN. Simulation results show that the proposed protocol performs better than other three compared routing protocols (AODV, DSDV and DSR) in package delivery rate (PDR) and end-to-end delay. Although the performance of FQMMP in overhead is not as good as the other three protocols, it is worthwhile for the emergency rescue.

Keywords: ECN; FQMM; FQMMP; Rescue Urgency Degree; post-earthquake

1. Introduction

After the devastating earthquake, emergency rescue crews are needed to rush to the scene for rescue as soon as possible. Post-earthquake emergency rescue includes material dispatching, team dispatching, personnel evacuation, post-disaster reconstruction, etc. Due to the different catastrophic degrees caused by the earthquake in different affected areas, the Rescue Urgency Degrees (RUDs) are different for those areas. Seismic intensity, which refers to the catastrophic degree of earthquake impact on the ground or artificial buildings in a certain area [1], can be used to express the rescue urgencies of disaster areas. The seismic intensity can be obtained in the following ways [2]: In the area where seismic observation equipment is intensively deployed, we can directly obtain the intensity distribution map of the instrument; In the area where seismic observation equipment is sparsely deployed, we can obtain the intensity distribution map of the instrument by grid interpolation; In the area where seismic observation equipment is rarely deployed, we can obtain the intensity distribution map either by historical seismic data statistics or earthquake simulations. Therefore, it is feasible to carry out emergency rescue according to the emergency degree of the disaster area reflected by seismic intensity.

After the devastating earthquake, the communication infrastructure and power system in the disaster area will suffer from different degrees of damage, resulting in communication system paralysis. Rescue crews have to quickly establish ECN in the disaster area to meet the communication demands both inside and outside the affected area.

Unlike traditional self-organized network, the nodes in ECN have the characteristics of energy limitation, high energy consumption in communication and low energy consumption in data calculation. In recent years, the research on ECN routing protocols has been widely concerned by scholars.

2. Related works

45 In the existing research on the mobility model of emergency rescue crews, the traditional task
46 assignment model, e.g., numerical type [3], time window [4] and linear time satisfaction function [5],
47 usually focuses on processing of rescue time. Song Ye et al. [6] established an optimization model
48 for the assignment of earthquake emergency rescue teams, aiming at improving rescue efficiency
49 and maximizing the satisfaction of rescue time. Pan Xinchao et al. [7] established an optimal
50 scheduling model for earthquake emergency rescue based on the precondition of rescue capability
51 constraints, expecting to treat as more wounded as possible in the shortest time. Li Mingyang et al.
52 [8] comprehensively considered the satisfaction of emergency rescue time and the competence of
53 rescue crews, and then established the dispatch and distribution model of emergency rescue crews,
54 which solved the dispatch problem of emergency rescue crews with multiple disaster areas. Li Jin et
55 al. [9] established a multi-resource and multi-disaster-point emergency scheduling model for
56 resource scheduling in emergency scenarios, and designed a heuristic algorithm based on network
57 optimization and linear programming optimization ideas in graph theory to reasonably schedule
58 disaster relief resources and minimize the loss of life and property. Cao Qingkui et al. [10] proposed
59 the experience satisfaction model of disaster victims to schedule the rescue crews, aiming at
60 obtaining the maximum experience satisfaction and the best rescue result. However, the above
61 researches studied the mobility models from the perspective of rescue capacity and relief materials
62 repertory, without considering seismic intensity in disaster areas. Furthermore, the above
63 researches did not reasonably allocate the communication and rescue nodes based on the
64 characteristics of ECN.

65 In the field of ECN protocol investigation, Li Mufeng et al. [11] studied the energy
66 consumption of nodes in emergency communication scenarios. Based on the DCHS (deterministic
67 cluster head selection) protocol, the link quality was introduced into the communication cost
68 function, and a shortest path non-uniform clustering algorithm based on link quality was proposed
69 to extend the lifetime of ECN by saving energy. Xue Lisi et al. [12] took Ya'an earthquake as an
70 example, established different earthquake emergency communication models in earthquake by
71 analyzing the topography of Sichuan Province, and screened out the multi-copy routing protocol
72 which was suitable for earthquake emergency communication in Sichuan Province. Yu Xiang et al.
73 [13] improved AODV protocol for emergency communication scenarios, and proposed SE-AODV
74 protocol which can reduce energy consumption and extend lifetime in ECN. Xiaoming Wang et al.
75 [14] proposed a two-stage extended forwarding dynamic routing protocol based on the degree of
76 social activity and physical contact factors of mobile users, which not only significantly improved
77 the delivery rate of messages, but also reduced the cost ratio and average delay of messages. In
78 ECN, the routing discovery process of on-demand routing protocol is expensive, and the energy
79 consumption of nodes is large. In order to solve the above problems, R. Ramalakshmi et al. [15]
80 proposed a weighted low-power routing protocol. The protocol selected the maximum weighted
81 and minimum connected control set of network nodes based on the weights, which consisted of
82 link stability, mobility and energy. Simulation results showed that the protocol was superior to
83 other protocols in packet delivery rate, control message overhead, transmission delay and energy
84 consumption. Dhafer Ben Arbia et al. [16] proposed a new multi-hop routing protocol for ECN,
85 through which an ad-hoc network between rescue crews and command center was established. The
86 routing table was optimized based on real-time end-to-end link quality estimation. Compared with
87 other routing protocols, the proposed protocol was superior in packet received rate and energy
88 consumption, which extended lifetime and enhanced reliability of ECN. Vipin bondre et al. [17], B.
89 Ramakrishnan et al. [18] analyzed the performance of AODV, DSR, DSDV and other traditional
90 routing protocols in emergency scenarios. However, they did not consider the mobility model of
91 rescuers, nor the *RUDs* (Rescue Urgency Degrees) in disaster areas.

92 In this paper, we first propose a seismic intensity based four-quadrant rescue mobility model
93 (FQMM), then we simulate earthquake scene and propose a FQMM-based protocol for ECN. The
94 main contributions of this paper are as follows:

95 Firstly, this paper gives the topology of ECN for the scene of post-earthquake emergency
96 rescue.

97 Secondly, the FQMM mobility model for post-earthquake emergency rescue crews is proposed,
98 which based on the topological structure of ECN.

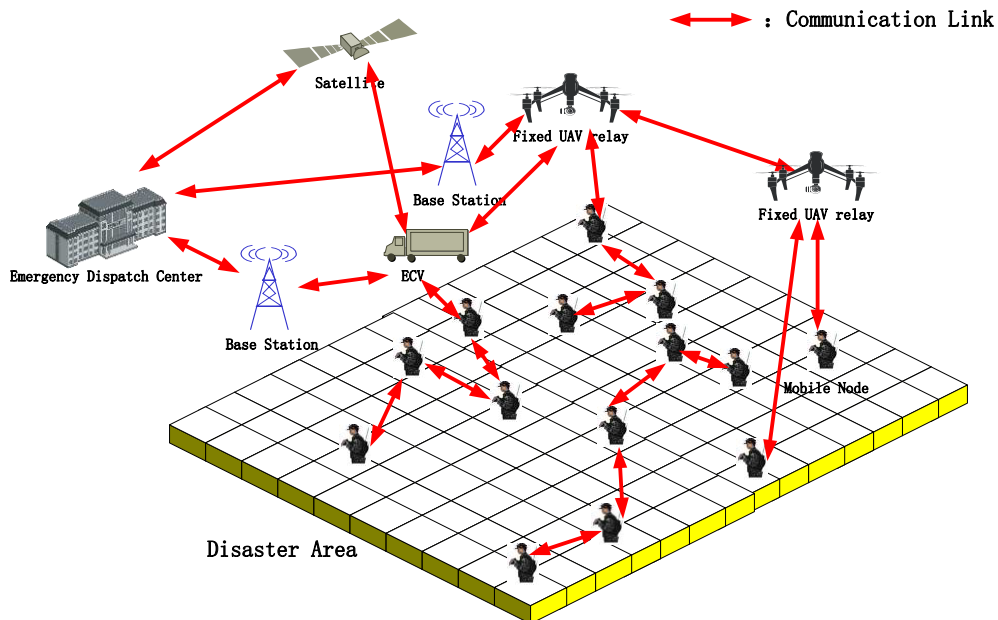
99 Finally, this paper proposes a FQMM-based protocol (FQMMP) for ECN. According to the
100 location of the mobile node, FQMMP predicts hop counts from source to destination, so that it can
101 update the routing table in real time by selecting the optimal next-hop node, thus improving
102 package delivery rate, reducing end-to-end delay.

103 Although the routing protocol proposed in this paper only considers the factor of seismic
104 intensity, the designed mobility model is universal and can be applied to other natural disasters,
105 such as floods, fires, typhoons and so on.

106 3. Method

107 3.1. Scenario and Assumptions

108 In the post-earthquake ECN, the emergency communication vehicle (ECV) and base station (BS)
109 are regarded as fixed nodes, while rescue crews equipped with individual communication
110 equipment are regarded as mobile nodes. Unmanned Aerial Vehicle (UAV) can be used not only as
111 a fixed node for relaying communication, but also as a mobile node for collecting disaster
112 information. A typical post-earthquake ECN is shown in Figure 1.



113 **Figure 1.** An example of post-earthquake ECN

114 After the earthquake, rescuers equipped with individual communication equipment were
115 scattered to various disaster areas for rescue. Each communication node in ECN, such as ECV, UAV
116 and portable individual equipment (PIE), has its own communication coverage. Since ECV cannot
117 reach the center of the disaster area due to traffic control, it starts at the midpoint of length, where
118 rescue crews start and stop rescue missions, as shown in Figure 2. In the rescue process, ECV can
119 provide real-time communication for rescue crews. Due to its mobility and air superiority, UAV can
120 go deep into the disaster area and play the role of communication relay or disaster information
121 collector. However, due to the limited battery capacity and high costs of UAV, we are unable to
122 deploy a large number of UAVs in the disaster area. Rescuers can enter the disaster area with PIE,
123 however, due to the limited coverage, high cost and large energy consumption, PIE cannot play the
124 role of hot spot or relay for a long time. Therefore, how to cooperate with the communication
125 equipment in ECN to improve the communication efficiency is one of the key issues that need to be
126 paid attention to in post-earthquake emergency rescue. Therefore, heterogeneous communication
127 devices in ECN need to cooperate with each other through appropriate routing protocols to
128 improve communication efficiency. The symbols used in this paper are listed in Table 1.

129
130

Table 1. Parameter definition and description

Parameters	Description
RUD	Rescue Urgency Degree, which is inversely proportional to the seismic intensity value in this area. The closer the area is to the epicenter, the lower the value of RUD is, which means the disaster is serious and the priority of rescue is high; Otherwise, the opposite. When $RUD = 1$, the epicenter disaster area is a rectangle; When $RUD > 1$, the disaster areas are rectangle rings that expands outwards in turn.
a_i	Length of area where $RUD=i$.
b_i	Width of area where $RUD=i$.
QL	Quadrant Level, which is the number of times the quadrant divided.
QID	Quadrant ID.
RT	Number of Rescue Tasks.
NRA	Number of Rescuers Allocated.
M	Number of mobile nodes.

132 After the earthquake, we use rectangle to represent the earthquake influence range. The length
 133 and width of the rectangle are a_i and b_i ($i=1\dots n$) respectively. Before studying the mobile model, we
 134 propose the following assumptions for simulation calculation:

135 **Assumption 1:** In the region with equal seismic intensity, the value of RUD is equal.

136 **Assumption 2:** Each rescuer has got equal rescue efficiency.

137 **Assumption 3:** Rescue tasks in low RUD areas are at high priority. Rescue crews cannot start rescue
 138 tasks in higher RUD areas until rescue tasks in low RUD areas are completed.

139 **Assumption 4:** Random waypoint mobility model [19] for rescuers is used in each disaster area. In
 140 order to ensure the fairness and rationality of the rescue sequence, the rescuers are approximately
 141 evenly distributed in disaster areas with equal RUD values.

142 **Assumption 5:** Locations and number of rescue tasks are known by rescue crews in advance, since
 143 the Global Positioning System (GPS) is used.

144 Based on seismic intensity and number of rescuers in disaster areas, this paper proposes a
 145 four-quadrant mobility model of rescue crews, which improves the rescue efficiency and ensures
 146 the safety of the victims' lives and properties. The proposed mobility model mainly includes two
 147 aspects: Firstly, the most seriously affected areas are rescued as soon as possible; secondly, the
 148 rescue crews are allocated to each appropriate quadrant, which improves the rescue efficiency and
 149 shortens the time of rescue.

150 3.2. Disaster area division

151 Disaster area is divided into n layers according to seismic intensity. The epicenter is located in
 152 the first layer ($RUD=1$) where length is a_1 and width is b_1 . We define RUD of each region as $1, 2, \dots, n$.
 153 Epicenter located at the center of rectangle where $RUD=1$. All areas are rectangular rings, except for
 154 the one with $RUD=1$, which is a rectangle. ECV parks at the midpoint of the length outside the
 155 rectangular ring with $RUD=n$, as shown in Figure 2.

156 The length and width of each disaster area are marked as $\{RUD | a_i, b_i\}$, then each region can be
 157 expressed as follows:

158 Region 1: $\{RUD=1 | a_1, b_1\}$;

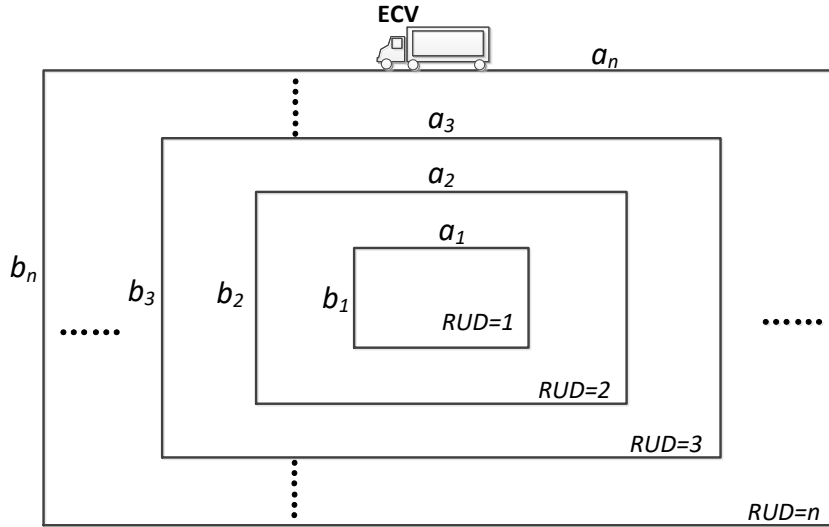
159 Region 2: $\{RUD=2 | a_2 = a_1 + \frac{a_1}{2} + \frac{a_1}{2} = 2a_1, b_2 = b_1 + \frac{b_1}{2} + \frac{b_1}{2} = 2b_1\}$;

160 Region 3: $\{RUD=3 | a_3 = a_2 + \frac{a_2}{2} + \frac{a_2}{2} = 2a_2 = 4a_1, b_3 = b_2 + \frac{b_2}{2} + \frac{b_2}{2} = 2b_2 = 4b_1\}$;

161 According to mathematical induction, we can get:

162 Region i : $\{RUD=i | a_i = 2a_{i-1} = 2^{i-1}a_1, b_i = 2b_{i-1} = 2^{i-1}b_1\}$.

163



164

165

Figure 2. Disaster area division according to RUD

166 **3.3. Four-quadrant mobility model (FQMM)**

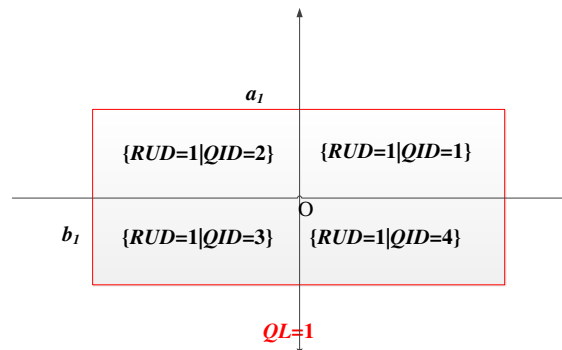
167 In this section, a four-quadrant rescuers allocation scheme is proposed. Based on this scheme, a
 168 four-quadrant mobility model (FQMM) for rescuers is proposed. The objectives of the allocation
 169 scheme are: 1) carrying out grid search in disaster areas to ensure the effectiveness of rescue
 170 without missing any victims; 2) carrying out radiation diffusion rescue from epicenter to ensure the
 171 worst affected areas are on top of the rescue list. From the disaster area division discussed in
 172 Section 3.2, it can be seen that when $RUD=1$, the region is a rectangle, and when $RUD>1$, the regions
 173 are rectangular rings. Therefore, the discussion of rescuers allocation scheme include two aspects:
 174 $RUD=1$ and $RUD>1$. The core ideas of rescuers allocation scheme for regions with $RUD>1$ are
 175 similar, though the lengths of the regions are different.

176 **3.3.1. Mobility model for rescuers in regions with $RUD=1$**

177 Five steps (**Step 1** to **Step 5**) are included in the mobility model of rescuers for regions with
 178 $RUD=1$.

179 **Step 1:** As shown in Figure 3, we establish a coordinate system which takes the epicenter as the
 180 origin. X and Y axes are the length and width of the rectangle. Four quadrants, $QID = 1$, $QID = 2$,
 181 $QID = 3$ and $QID = 4$ are counter-clockwise defined according to the definition of coordinate system.
 182 Each quadrant is described as follows:

183 Quadrant 1: $\{RUD=1 | QID = 1\}$; Quadrant 2: $\{RUD=1 | QID = 2\}$; Quadrant 3: $\{RUD=1 | QID = 3\}$;
 184 Quadrant 4: $\{RUD=1 | QID = 4\}$.



185

186

Figure 3. Disaster area with $RUD=1$ is divided into 4 quadrants for the first time ($QL=1$)

187 Suppose that the total number of rescuers is M , and the total number of rescue tasks in the area
 188 with $RUD = 1$ is Q , which is, $RT_{QL=0}^{RUD=1} = Q$, where $RT_{QL=0}^{RUD=1}$ stands for total number of rescue tasks
 189 to be completed in disaster areas with $RUD=1$ and $QL=0$. The number of tasks to be performed in
 190 each quadrant is described as: $RT_{QID=k}^{RUD=1} = [Q/4]$, ($k = 1, 2, 3, 4$), where $RT_{QID=k}^{RUD=1}$ stands for
 191 the number of tasks to be performed in disaster areas with $RUD=1$ and $QID=k$ ($k=1, 2, 3, 4$). Rescuers
 192 are evenly allocated to four quadrants with $QL=1$, and the number of rescuers allocated (NRA) in
 193 each quadrant can be discussed from four cases (**Case 1 to Case 4**) as follows:

194 **Case 1:** $\text{Mod}[M/4]=0$, where function $\text{Mod}[x/y]$ is used to return the remainder of the division
 195 of two numbers x, y . In this case, a quarter of rescuers are evenly allocated to four quadrants with
 196 $QL=1$, which is:

$$197 \quad NRA_{QID=k}^{RUD=1} = \frac{M}{4}, \quad (k = 1, 2, 3, 4)$$

198 where $NRA_{QID=k}^{RUD=1}$ stands for the number of rescuers allocated in each quadrant with $RUD=1$ and
 199 $QID=k$.

200 **Case 2:** $\text{Mod}[M/4]=1$. In this case, one more rescuer is allocated to Quadrant 1, which are:

$$201 \quad NRA_{QID=1}^{RUD=1} = \frac{M-1}{4} + 1$$

$$202 \quad NRA_{QID \neq 1}^{RUD=1} = \frac{M-1}{4}$$

203 where $NRA_{QID=1}^{RUD=1}$ stands for the number of rescuers allocated in Quadrant 1 with $RUD=1$, and
 204 $NRA_{QID \neq 1}^{RUD=1}$ stands for the number of rescuers allocated in Quadrant 2, Quadrant 3 and Quadrant 4
 205 with $RUD=1$.

206 **Case 3:** $\text{Mod}[M/4]=2$. In this case, one more rescuer is allocated to Quadrant 1 and Quadrant 2
 207 respectively, which are:

$$208 \quad NRA_{QID=1 \text{ or } 2}^{RUD=1} = \frac{M-2}{4} + 1$$

$$209 \quad NRA_{QID=3 \text{ or } 4}^{RUD=1} = \frac{M-2}{4}$$

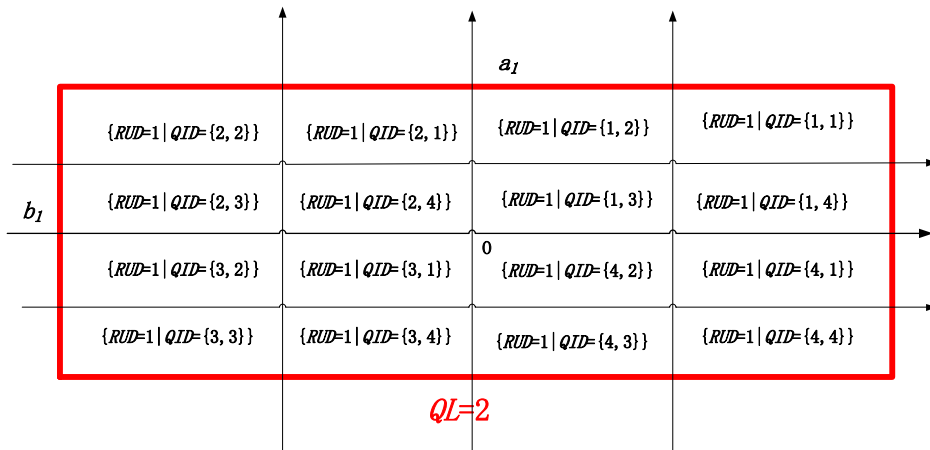
210 where $NRA_{QID=1 \text{ or } 2}^{RUD=1}$ stands for the number of rescuers allocated in Quadrant 1 and Quadrant 2
 211 with $RUD=1$, and $NRA_{QID=3 \text{ or } 4}^{RUD=1}$ stands for the number of rescuers allocated in Quadrant 3 and
 212 Quadrant 4 with $RUD=1$.

213 **Case 4:** $\text{Mod}[M/4]=3$. In this case, one more rescuer is allocated to Quadrant 1, Quadrant 2,
 214 Quadrant 4, which are:

$$215 \quad NRA_{QID \neq 3}^{RUD=1} = \frac{M-3}{4} + 1$$

$$216 \quad NRA_{QID=3}^{RUD=1} = \frac{M-3}{4}$$

217 where $NRA_{QID \neq 3}^{RUD=1}$ stands for the number of rescuers allocated in Quadrant 1, Quadrant 2 and
 218 Quadrant 4 with $RUD=1$, and $NRA_{QID=3}^{RUD=1}$ stands for the number of rescuers allocated in Quadrant 3
 219 with $RUD=1$.



220

221

Figure 4. Disaster area with $RUD=1$ is divided into 16 quadrants for the second time ($QL=2$)

222 **Step 2:** According to the procedure of step 1, each quadrant with $RUD=1$ is further divided into
 223 four secondary quadrants as shown in Figure 4. Two elements are included in QID set, which
 224 record the quadrant ID from the first level to the last level. For example, $\{RUD=1|QID=\{1,3\}\}$ in
 225 Figure 4 means region with $QL=1$ is located in Quadrant 1 and region with $QL=2$ is located in
 226 Quadrant 3.

227 **Step 3:** For $QL=x$, replace the value of M with $RT_{QL=x}^{RUD=1}$, repeat Step 1 and calculate the number
 228 of rescuers allocated for each quadrant with $QL=x$.

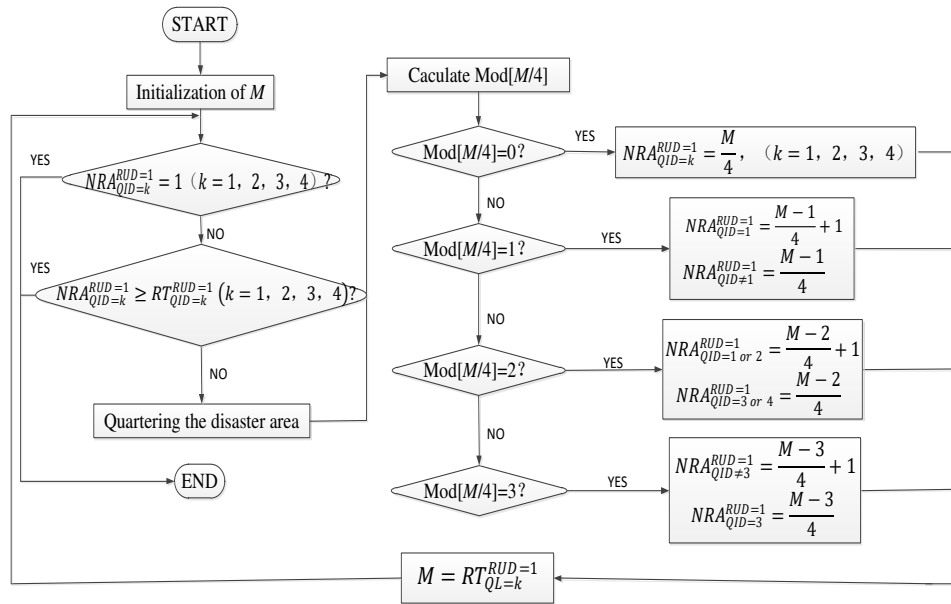
229 **Step 4:** Repeat **Step 2** and **Step 3**, until any of the following **Abort Conditions** is satisfied.

230 **Abort Condition 1:** There is only one rescuer in each area of quadrant with $QL=x$, which
 231 is: $NRA_{QID=k}^{RUD=1} = 1$, ($k = 1, 2, 3, 4$), where $NRA_{QID=k}^{RUD=1}$ is the number of rescuers allocated in
 232 Quadrant k ($k=1, 2, 3, 4$) with $RUD=1$ and $QL=x$. Under this condition, further quadrant division is
 233 no longer meaningful, so the single rescuer will complete all rescue tasks in the region of quadrant
 234 with $QL=x$.

235 **Abort Condition 2:** The number of rescue tasks is less than that of rescuers assigned in the
 236 quadrant with $QL=x$, which is: $NRA_{QID=k}^{RUD=1} \geq RT_{QID=k}^{RUD=1}$, ($k = 1, 2, 3, 4$), where $NRA_{QID=k}^{RUD=1}$ is the
 237 number of rescuers allocated in Quadrant k ($k=1, 2, 3, 4$) with $RUD=1$ and $QL=x$, and $RT_{QID=k}^{RUD=1}$ is
 238 number of rescue tasks in Quadrant k ($k=1, 2, 3, 4$) with $RUD=1$ and $QL=x$. Under this condition,
 239 each rescuer is assigned to at most one rescue task, and there are unoccupied rescuers in the area.

240 **Step 5:** Quadrant division is suspended and rescuers begin to perform their own rescue tasks.

241 Figure 5 shows the algorithm flow of rescue node allocation in rectangular disaster area when
 242 $RUD = 1$.



243

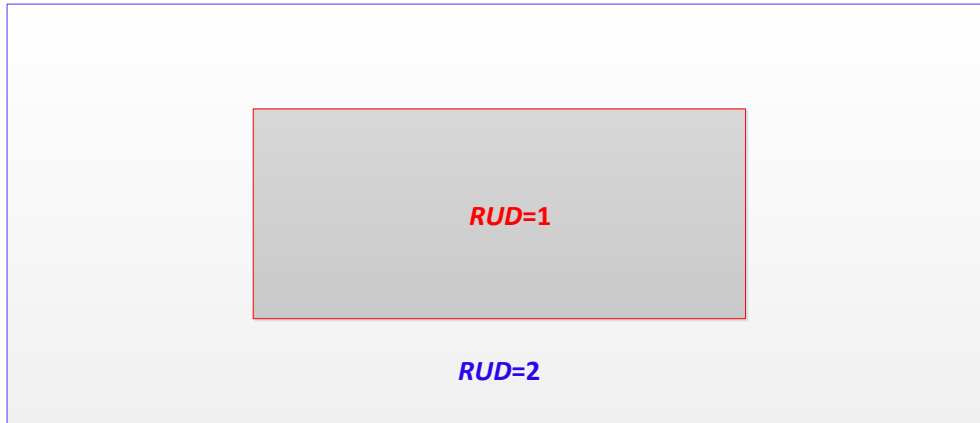
244

Figure 5. Allocation process of rescue nodes in disaster area with $RUD=1$

245 3.3.2. Mobility model for rescuers in regions with $RUD>1$

246 According to the mobility model, rescue crews cannot start rescue tasks in higher RUD areas
 247 until rescue tasks in low RUD areas are completed. As shown in Figure 6, in the gray area with
 248 $RUD=1$, rescuers are carrying out rescue tasks. When the task is over, rescuers will be assigned to
 249 the white rectangular ring area with $RUD=2$.

250 Five steps (**Step 6** to **Step 10**) are included in the mobility model of rescuers for regions with
 251 $RUD>1$.



252

253

Figure 6. Rectangular ring with $RUD > 1$

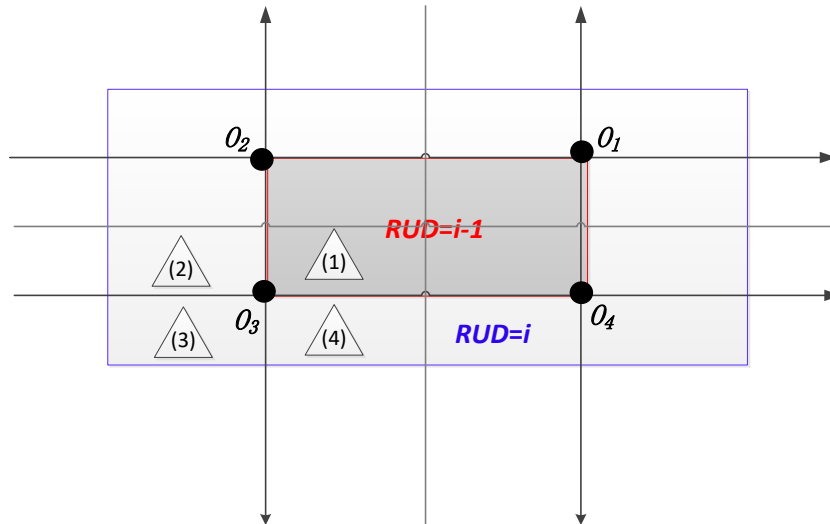
254

255

256

257

Step 6: As shown in Figure 7, we establish four coordinate systems which takes O_1 , O_2 , O_3 and O_4 as the origins respectively. Then the rectangular ring is equally divided into twelve quadrants (the white parts in Figure 7) by four coordinate systems. In each coordinate system, four quadrants are equal with each other in area, as shown in Figure 7 where four triangle marks.



258

259

Figure 7. Disaster area with $RUD > 1$ is divided into 12 quadrants for the first time ($QL=1$)

260

261

262

263

264

265

266

267

268

269

270

271

272

Step 7: It can be seen from **Step 6** that in each coordinate system, there are three quadrants waiting for allocation of rescuers, and the left quadrant is allocated with rescue crews. As shown in Figure 7, in the coordinate system with O_3 as origin, there are four quadrants where Triangle (1), Triangle (2), Triangle (3) and Triangle (4) marks. Area where Triangle (1) marks is allocated with rescue crews, while areas where Triangle (2), Triangle (3) and Triangle (4) marks are waiting for rescuers allocations. We take coordinate system O_3 as an example. Suppose there are M rescuers in Quadrant 1 with $RUD=i-1$, which marked with Triangle (1). There are Q rescue tasks in areas with $RUD=i$, which is: $RT_{QL=0}^{RUD=i} = Q$. Rescuers are evenly allocated to three quadrants (Triangle (2), Triangle (3) and Triangle (4)) with $QL=1$, and the number of rescuers allocated (NRA) in each quadrant can be discussed from three cases (**Case 5 to Case 7**) as follows:

Case 5: $\text{Mod}[M/3]=0$, where function $\text{Mod}[x/y]$ is used to return the remainder of the division of two numbers x, y . In this case, one-third rescuers are evenly allocated to three quadrants, which is:

273

$$NRA_{QID=k}^{RUD=i} = \frac{M}{3}, \quad (k = 2, 3, 4)$$

274 where $NRA_{QID=k}^{RUD=i}$ stands for the number of rescuers allocated in each quadrant with $RUD=i$ and
 275 $QID=k$.

276 **Case 6:** $\text{Mod}[M/3]=1$. In this case, one more rescuer is allocated to Quadrant 2, which are:

$$277 \quad NRA_{QID=2}^{RUD=i} = \frac{M-1}{3} + 1$$

$$278 \quad NRA_{QID=3 \text{ or } 4}^{RUD=i} = \frac{M-1}{3}$$

279 where $NRA_{QID=2}^{RUD=i}$ stands for the number of rescuers allocated in Quadrant 2 with $RUD=i$, and
 280 $NRA_{QID=3 \text{ or } 4}^{RUD=i}$ stands for the number of rescuers allocated in Quadrant 3 and Quadrant 4 with
 281 $RUD=i$.

282 **Case 7:** $\text{Mod}[M/3]=2$. In this case, one more rescuer is allocated to Quadrant 2 and Quadrant 4
 283 respectively, which are:

$$284 \quad NRA_{QID=2 \text{ or } 4}^{RUD=i} = \frac{M-2}{3} + 1$$

$$285 \quad NRA_{QID=3}^{RUD=i} = \frac{M-2}{3}$$

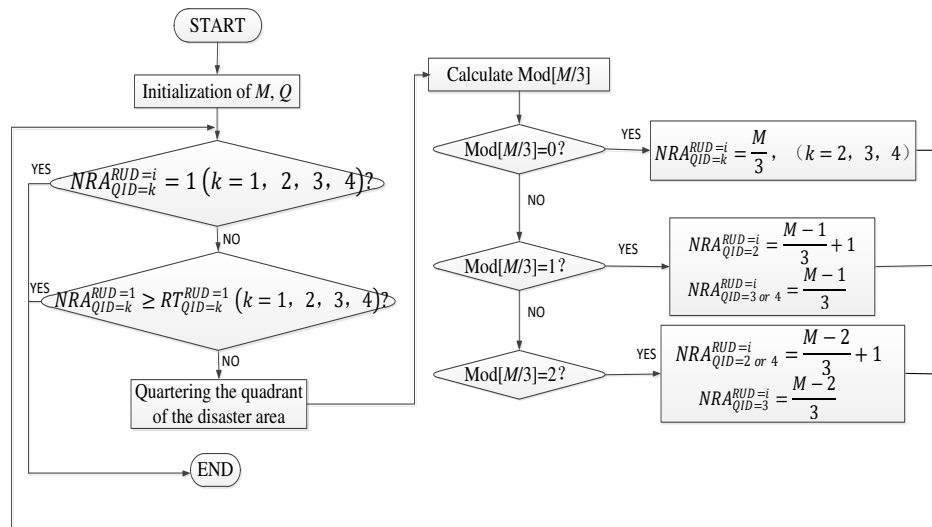
286 where $NRA_{QID=2 \text{ or } 4}^{RUD=i}$ stands for the number of rescuers allocated in Quadrant 2 and Quadrant 4
 287 with $RUD=i$, and $NRA_{QID=3}^{RUD=i}$ stands for the number of rescuers allocated in Quadrant 3 with $RUD=i$.
 288 The number of rescue tasks in each quadrant with $RUD=i$ is: $RT_{QID=k}^{RUD=i} = [Q/12]$, ($k = 2, 3, 4$),
 289 where $RT_{QID=k}^{RUD=i}$ stands for the number of rescue tasks in Quadrant k ($k=2, 3, 4$) with $RUD=i$.

290 **Step 8:** Quadrants ($QL \geq 2$) division methods are the same as illustrated in **Step 6**, which take
 291 the middle points of quadrants with $QL=1$ as the origins and establish the coordinate systems.
 292 Repeat **Step 7**, until any of the following **Abort Conditions** is satisfied.

293 **Abort Condition 3:** There is only one rescuer in each area of quadrant with $QL=x$, which
 294 is: $NRA_{QID=k}^{RUD=i} = 1$, ($k = 1, 2, 3, 4$), where $NRA_{QID=k}^{RUD=i}$ is the number of rescuers allocated in
 295 Quadrant k ($k=1, 2, 3, 4$) with $RUD=i$ and $QL=x$. Under this condition, further quadrant division is
 296 no longer meaningful, so the single rescuer will complete all rescue tasks in the region of quadrant
 297 with $QL=x$.

298 **Abort Condition 4:** The number of rescue tasks is less than that of rescuers assigned in the
 299 quadrant with $QL=x$, which is: $NRA_{QID=k}^{RUD=i} \geq RT_{QID=k}^{RUD=i}$, ($k = 1, 2, 3, 4$), where $NRA_{QID=k}^{RUD=i}$ is the
 300 number of rescuers allocated in Quadrant k ($k=1, 2, 3, 4$) with $RUD=i$ and $QL=x$, and $RT_{QID=k}^{RUD=i}$ is
 301 number of rescue tasks in Quadrant k ($k=1, 2, 3, 4$) with $RUD=i$ and $QL=x$. Under this condition, each
 302 rescuer is assigned to at most one rescue task, and there are unoccupied rescuers in the area.

303 **Step 9:** Quadrant division is suspended and rescuers begin to perform their own rescue tasks.



304

305 **Figure 8.** Allocation process of rescue nodes in disaster area with $RUD > 1$

306 Figure 8 shows the algorithm flow of rescue node allocation in rectangular disaster area when
 307 $RUD > 1$.

308 4. FQMM-based routing protocol

309 4.1. backgrounds

310 Post-earthquake ECN, which is a hybrid self-organized network, mainly includes ECV, UAV,
311 portable devices carried by rescue crews, base station, satellite, etc. Those communication devices
312 and be classified as fixed communication nodes (such as ECV, base station, UAV used for relay, etc.)
313 and mobile communication nodes (such as portable devices carried by rescue crews, satellite, etc.).
314 As shown in Figure 1, each portable device is equipped with a wireless communication module.
315 Rescuers can use portable devices to build self-organized networks, through which they can
316 communicate with each other and complete the transmission process of data packets, such as
317 receiving, transmitting and relaying. Rescuers can also communicate with ECV, UAV and other
318 fixed nodes within the coverages of portable devices. As a fixed communication node, ECV can
319 communicate with rescuers and UAVs in the disaster area through downlink, or with the base
320 station, satellite and other communication facilities through uplink. Through the backbone network,
321 commanders can get the information about rescue crews, rescue process and suffering condition in
322 time, so as to make scientific rescue decision and emergency response quickly.

323 We define the communication radius of mobile node as R . The mobile node sends data to the
324 emergency communication vehicle in the way of multi-hop. In such communication mode, the
325 source is the mobile node in the disaster area, the destination is ECV at the edge of the disaster area,
326 and the relay nodes are mobile nodes or fixed nodes (UAVs, etc.) in the disaster area. On the
327 premise of ensuring the stability of communication links, we choose relay nodes or links that can
328 minimize the delay for data transmission. Based on the mobility model we discussed in Section 3.3,
329 it can be seen that rescue crews are nearly evenly distributed in disaster areas with the same RUD .
330 In order to ensure the stability of the communication link in the rescue process, we place fixed
331 UAVs at the edges of disaster areas with different RUD values; however, they do not undertake the
332 rescue tasks. When all rescue tasks in the disaster area with a specific RUD value are completed, the
333 relay UAV in the area returns to the location of ECV.

334 4.2. Protocol design

335 In this section, a proposal of FQMM-based protocol (FQMMBP) for ECN is presented. First, we
336 discuss route discovery and maintenance of FQMMBP, and then we propose FQMMBP protocol by
337 analyzing the communication mechanism of nodes in ECN.

338 4.2.1. Route discovery and maintenance

339 In order to reduce the data transmission delay, we select the next hop relay node according to
340 RUD value, QL and QID of each region where mobile nodes are located in. RUD and QL are used to
341 define the level of the region where mobile nodes are located in. QID is a set which includes 1, 2, 3
342 and 4, and there are QL elements in the set. According to the set, the mobile nodes learn the division
343 of the regions and the quadrants position, so as to select the appropriate next hop mobile node.
344 Therefore, in the process of routing discovery, it is necessary to extend the routing request (RREQ)
345 message, so as to meet the requirements of our proposed communication mechanism of FQMMBP.
346 We improved the traditional RREQ message by adding four new fields: RUD , QL , QID and QW .
347 RUD describes the area where nodes are located and judge whether the area is a rectangle or a
348 rectangular ring as shown in Figure 2. QL describes the level of the quadrant where nodes are
349 located, and it determines the relative position of the mobile rescue node. QID describes the
350 division of the quadrant where nodes are located and judge its relative position to ECV. When the
351 QL of quadrants are the same, QID helps pick up the mobile rescue node which is closer to ECV.
352 QW calculates weights of nodes according to QL and QID , so as to select the most appropriate
353 next-hop relay node.

354 In the process of route discovery, nodes broadcast RREQ messages to send request information
355 to their neighbors. The improved RREQ data format is shown in Table 2.

356 Each field of RREQ data format is described as follows:
357 Type: The length of this field is 8bit, and the type value of RREQ is 1
358 Flags: The length of this field is 5 bits, and five identities (J, R, G, D, and U) are included in this
359 field. "J" is a joint flag and is generally used for multicast. "R" is for route repairing and is used for
360 multicast transmission. "G" represents the list of nodes around ECV which can be communicated.
361 Flag "G" determines whether the RREQ message can be directly sent to the destination or not. "D"
362 is the reply flag of the destination node which determines whether the destination node is allowed
363 to reply to the received RREQ message or not. "U" is the flag of unknown serial number. U=1
364 means that the serial number of the node is unknown.
365 Reserved: Reserved field for further improvement of RREQ message.
366 Hop Count: This field registers the hop counts that RREQ passes from the source node to the
367 current node.
368 RREQ ID: This field is the unique identity of RREQ message.
369 RUD: Rescue Urgency Degree, which is inversely proportional to the seismic intensity value in
370 this area.
371 QL: Quadrant Level, which is the number of times the quadrant divided.
372 QID: Quadrant ID.
373 QW: Weights of nodes in quadrant.
374

Table 2. The improved RREQ data format.

Type	Flags					Reserved	Hop Count
	J	R	G	D	U		

RREQ ID

Destination IP Address

Destination Sequence Number

Source IP Address

Source Sequence Number

RUD

QL

QID

QW

375 4.2.2. Communication mechanism of mobile node

376 As shown in Table 2, for fixed UAV nodes located in different *RUD* areas, all fields of RREQ
377 message are empty except for "*RUD*". The "*RUD*" field describes the UAV's location. Suppose that
378 there is one UAV relay node in each region with $RUD=i$ ($i=1$ to n), and the UAVs in two adjacent
379 regions can communicate with each other directly. Then there are $n + 1$ fixed communication nodes
380 in the disaster area (n fixed UAVs and one ECV). Mobile nodes in regions with $RUD=i$ ($i=1$ to n) can
381 transmit data to the fixed UAV node either by one hop or by multiple hops. After that, the data can
382 be transmitted to ECV through multi-hop between fixed nodes without relying on other mobile
383 nodes. In that case, we need to select the most appropriate next hop relay node (mobile node or
384 fixed node) when the next hop candidate is in different quadrants. It can be seen from Figure 2 that
385 Quadrant 1 and Quadrant 2 are closer to ECV than Quadrant 3 and Quadrant 4, so the weights of
386 Quadrant 1 and Quadrant 2 should be greater than that of Quadrant 3 and Quadrant 4. As shown in
387 Figure 9, the distance between the center of each quadrant and ECV is:

$$388 D_{QID} = \begin{cases} c & QID = 1 \text{ or } 2 \\ d & QID = 3 \text{ or } 4 \end{cases} \quad (1)$$

389

$$c = \sqrt{\left(\frac{a}{4}\right)^2 + \left(\frac{b}{4}\right)^2} \quad (2)$$

390

$$d = \sqrt{\left(\frac{a}{4}\right)^2 + \left(\frac{3b}{4}\right)^2} \quad (3)$$

391

392

393

394

395

396

397

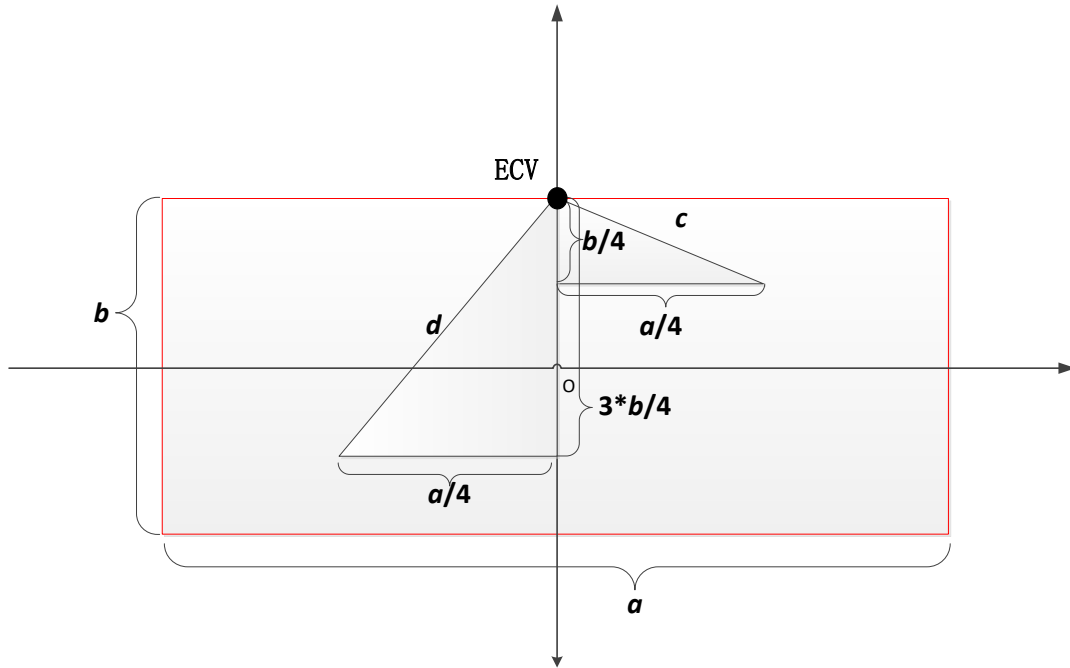
where a , b are length and width of disaster area respectively. D_{PH} stands for the distance between the center of each quadrant and ECV. c is the distance between the center of Quadrant 1 and ECV, which equals with the distance between the center of Quadrant 2 and ECV. d is the distance between the center of Quadrant 3 and ECV, which equals with the distance between the center of Quadrant 4 and ECV. Take the weight of Quadrant 1 (or Quadrant 2) as the benchmark, which is: $W_{QID=1 \text{ or } 2} = 1$, where $W_{QID=1 \text{ or } 2}$ is the weight of Quadrant 1 or Quadrant 2. The weight of Quadrant 3 (or Quadrant 4) can be expressed as:

398

$$W_{QID=3 \text{ or } 4} = \frac{d}{c} = \frac{\sqrt{a^2+9b^2}}{\sqrt{a^2+b^2}} \quad (4)$$

399

where $W_{QID=3 \text{ or } 4}$ is the weight of Quadrant 3 or Quadrant 4.



400

401

Figure 9. Calculate the weight of each quadrant according to the distance from quadrant center to ECV

402

Definition: QID_i is the Quadrant ID with $QL=i$. For example, $QID_3 = 4$ means Quadrant 4 is with $QL=3$. From Eq.(1) and Eq.(4), we can get:

403

404

$$D_{QID_i} = \begin{cases} c_i & QID_i = 1 \text{ or } 2 \\ d_i & QID_i = 3 \text{ or } 4 \end{cases} \quad (5)$$

405

406

407

408

409

where D_{QID_i} stands for the distance between the center of quadrant with QID_i and ECV. c_i is distance between the center of Quadrant 1 with $QL=i$ and ECV, which equals with the distance between the center of Quadrant 2 with $QL=i$ and ECV. d_i is distance between the center of Quadrant 3 with $QL=i$ and ECV, which equals with the distance between the center of Quadrant 4 with $QL=i$ and ECV. From Eq.(4), we can get:

410

$$W_{QID_i} = \frac{\sqrt{a_i^2+9b_i^2}}{\sqrt{a_i^2+b_i^2}} \quad (6)$$

411

412

413

414

where W_{QID_i} is the weight of node located in Quadrant QID_i . a_i , b_i are length and width of disaster area with $QL=i$ respectively. According to the QID and QL , we can get the total weight of each node in quadrants with different levels by:

415

$$QW = \sum_{i=1}^{QL} W_{QID_i} \quad (7)$$

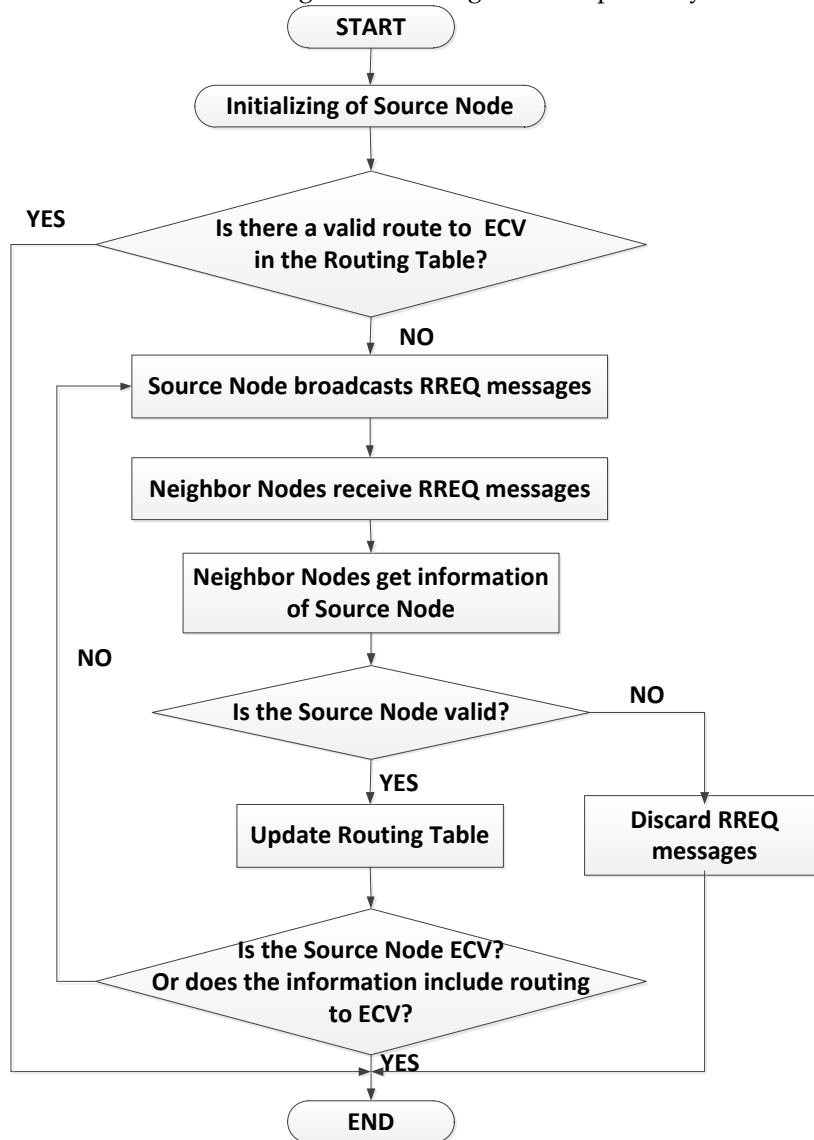
416

where QW is the total weight of one node in quadrants with different levels. W_{QID_i} is the weight of node located in Quadrant QID_i .

417 Suppose two nodes are located in Quadrant 1 and Quadrant 2 respectively, and the QW values
 418 of the two nodes are equal. According to FQMM, there is a higher probability that more rescuers
 419 are allocated in Quadrant 1 than in Quadrant 2. In that case, it is better to choose next hop nodes in
 420 Quadrant 1 than in Quadrant 2, because the probability of connecting to the destination node is
 421 higher. As a result, the priority of each quadrant is as follows: Quadrant 1 > Quadrant 2 > Quadrant
 422 4 > Quadrant 3. When the QW values of the nodes are equal, we can choose the node in the high
 423 priority quadrant as the next hop node.

424 4.2.3. FQMMBP design

425 In this section, we propose FQMMBP protocol based on FQMM. Routing discovery and routing
 426 maintenance process are illustrated in Figure 10 and Figure 11 respectively.



427
 428 **Figure 10.** Routing establishment process for FQMMBP

429 As shown in Figure 10, source node (denoted as N_s) checks whether there is a route to ECV. If
 430 there is no route to ECV, the node broadcasts RREQ message to its neighbor node (denoted as N_N).
 431 After receiving the message, N_N first checks whether N_s is a valid node. If N_s is invalid, N_N discards
 432 the received RREQ message; otherwise, N_N updates the routing table and finds out whether there is
 433 routing information to ECV. If there is no route to ECV, N_N forwards the received RREQ message.
 434 Repeat the broadcasting and checking process until one or more valid routes to the ECV are found.

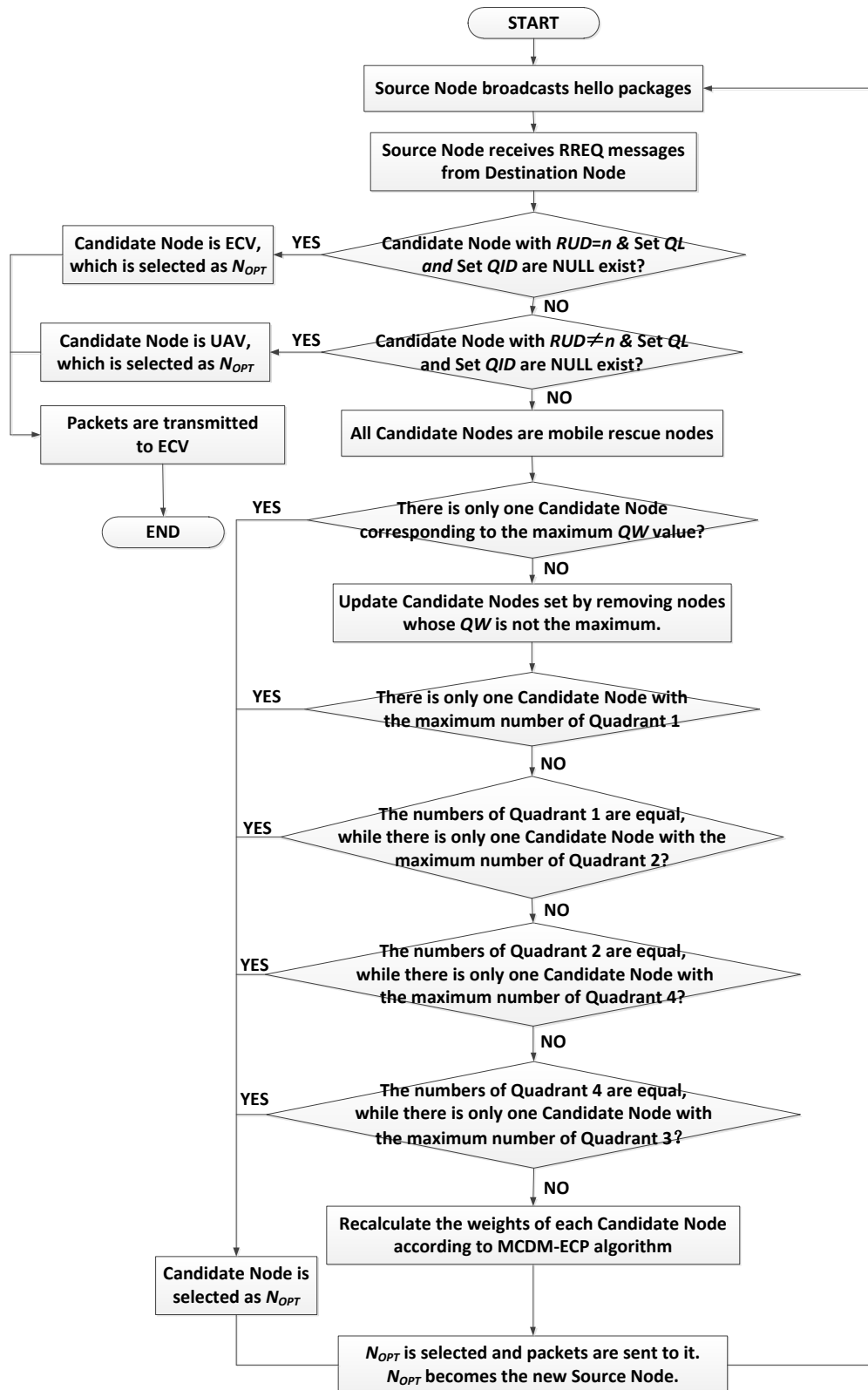


Figure 11. Routing maintenance process for FQMMBP

435
436
437
438
439
440
441
442
443

As shown in Figure 11, source node (denoted as N_s) sends *hello* packets to the candidate nodes within its coverage by broadcasting, and receives RREQ replies from them. N_s determines whether there is a RREQ reply sent by ECV by checking whether there is a candidate node with $RUD=n$ and both QL and QID are empty in RREQ reply. If there is an ECV within the coverage of N_s , data packets are directly transmitted to ECV which is the destination of the communication, and communication ends. If there is no ECV within the coverage of N_s , then N_s determines whether there is a RREQ reply sent by fixed UAV by checking whether there is a candidate node with

444 $RUD \neq n$ and both QL and QID are empty in RREQ reply. If there is an UAV within the coverage of
 445 N_s , data packets are forwarded to UAV, and UAV forwarded data packets to its neighbor. Repeat
 446 this process until ECV is founded, finally communication ends. If there are neither ECVs nor UAVs
 447 in the candidate nodes, we compare QW values. If there is only one candidate node corresponding
 448 to the maximum QW value, then this node is the optimal next hop node (denoted as N_{OPT}). N_{OPT}
 449 becomes a new source node N_s , and then it sends the *hello* packets to repeat the process. If the
 450 maximum QW value corresponds to more than one candidate nodes, we should update candidate
 451 nodes set by removing nodes whose QW is not the maximum. After that, we select N_{OPT} from the
 452 new set according to the following **Cases**:

453 **Case 1:** There is only one candidate node with the maximum number of Quadrant 1. This node is
 454 selected as N_{OPT} .

455 **Case 2:** The numbers of Quadrant 1 are equal, while there is only one candidate node with the
 456 maximum number of Quadrant 2. This node is selected as N_{OPT} .

457 **Case 3:** The numbers of Quadrant 2 are equal, while there is only one candidate node with the
 458 maximum number of Quadrant 4. This node is selected as N_{OPT} .

459 **Case 4:** The numbers of Quadrant 4 are equal, while there is only one candidate node with the
 460 maximum number of Quadrant 3. This node is selected as N_{OPT} .

461 **Case 5:** Recalculate the weights of each candidate node according to MCDM-ECP algorithm [20]
 462 and then select N_{OPT} .

463 The description of FQMMBP routing maintenance process is completed.

464 5. Experiment

465 In this section we present the network level performance evaluation and simulations results of
 466 the proposed routing protocol based on NS-2 platform. For comparison, with the respect to each
 467 relevant class of routing protocols, we selected the pertinent protocols which are the most widely
 468 used (e.g., AODV[17], DSR[18], DSDV[18]).

469 5.1. Simulation Setup

470 The simulation environment is a $10km \times 10km$ earthquake disaster area, in which the epicenter
 471 of the most severely affected area is $6km \times 4km$. There are 48 mobile rescue nodes, two fixed UAVs
 472 and one ECV. The simulation setup and respective parameters are detailed in Table 3.

473 **Table 3.** Simulation Parameters.

Parameters	Values
Number of mobile rescue nodes (M)	48
Fixed communication nodes (ECV included)	3
Simulation time span	600s
Area of earthquake affected regions	$10km \times 10km$
a_1	$6km$
b_1	$4km$

474 5.2. Simulation Results

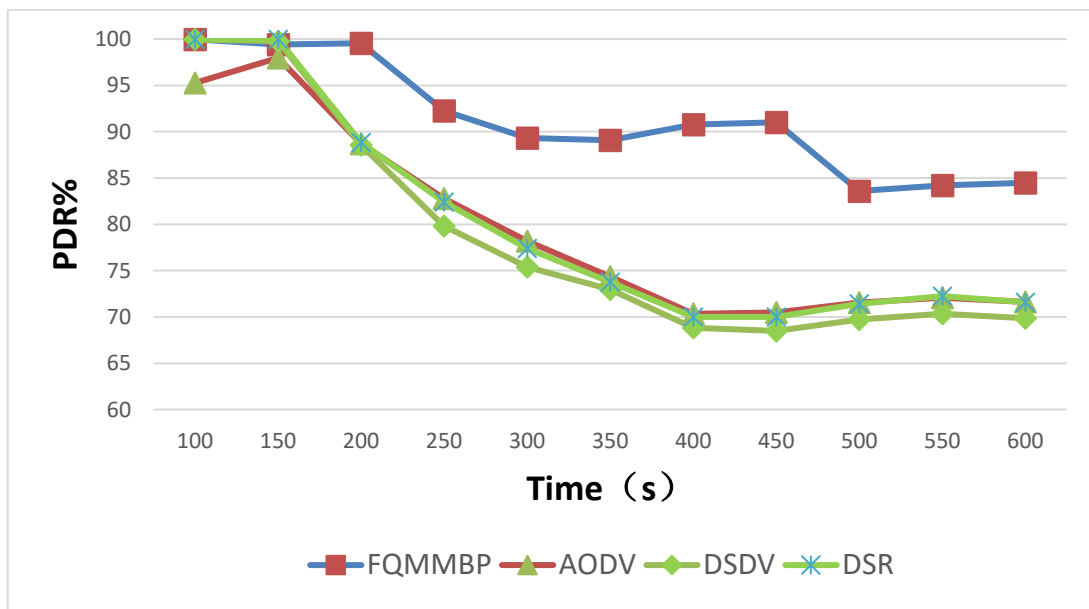
475 In this section, four routing protocols, e.g., FQMMBP, AODV, DSDV and DSR are analyzed
 476 from the perspective of package delivery rate (PDR), end-to-end delay (delay) and overhead.

477 5.2.1. Package Delivery Rate

478 Figure 12 shows the performance of Package Delivery Rate (PDR) for the different studied
 479 protocols. Our proposed FQMMBP achieves the best performance with nearly 91.24% of average
 480 PDR while the other three protocols with about 80% of average PDR. This proves that FQMMBP
 481 improves communication efficiency and stabilizes communication link status in a long period of
 482 time. DSDV achieves the worst performance with 79.23% of average PDR mainly due to the
 483 mobility of communication nodes. DSDV is a proactive protocol and each node maintains a route

484 table. In the emergency rescue scenario, routing tables are dynamic due to the mobility of rescuers,
 485 thus causing the cost of maintaining routing tables. The superiority of FQMMBP over other three
 486 routing protocols is mainly attributed to FQMM mobility model. In each disaster area under this
 487 model, the distribution of rescue mobile nodes tends to be uniform, which increases the probability
 488 that each node can find the appropriate next-hop node to forward data, and ensures the integrity
 489 and reliability of communication link. Packets are likely to be delivered successfully in such
 490 distributions of nodes.

491 PDR performances of the four compared protocols are almost the same before 150s, that is
 492 because all nodes are concentrated in the central area with $RUD=1$ at the beginning of simulation.
 493 At this point, the distributions of nodes in the four protocols are similar, and each node has not
 494 started to disperse or move to the next area according to the mobility model. As time goes on, the
 495 PDR of each protocol decreases gradually. This is because when the nodes complete the rescue
 496 tasks in the central area, they will spread to the next peripheral rectangular ring, resulting in the
 497 scattered distribution of nodes and the increase of distance between nodes, so the stability of
 498 communication link becomes poor. On the contrary, mobile nodes are evenly distributed and close
 499 to ECV under our proposed FQMMBP, which improves PDR.
 500



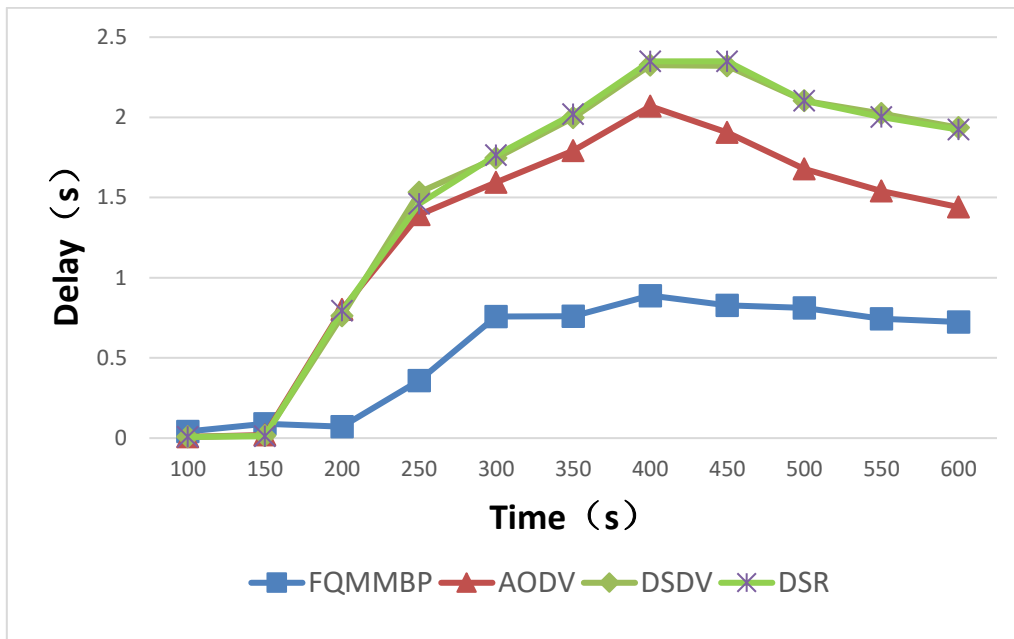
501
 502 **Figure 12.** Comparison of packet delivery rate (PDR) for four protocols

503 **5.2.2. End-to-end delay**

504 Figure 13 shows the performance of End-to-end delay (delay) for the different studied
 505 protocols. In terms of delay, FQMMBP is significantly lower than other classical routing protocols.
 506 During the simulation, the average delay decreased from 1.44s of DSR to 0.55s of FQMMBP, which
 507 proves the significant improvement of communication performance. This is because in each rescue
 508 area, the distribution of mobile nodes tends to be uniform under FQMMBP, which increases the
 509 probability that each node can find the next hop node to communicate with. Within the coverage of
 510 each relay node, the existence probability of candidate next hop node increases, which shortens the
 511 time to find the candidate next hop node as well as the time to transmit data to ECV.

512 Performances of four compared protocols are almost the same before 150s. This is because at
 513 the beginning of the simulation, all nodes are concentrated in the central rectangular area with the
 514 most serious seismic intensity. At this time, the distributions of nodes are relatively centralized and
 515 similar, and the nodes have not started to disperse and move according to their respective mobility
 516 models, so the performance differences of the four protocols are not significant. As time goes on, the
 517 delay of each protocol increases gradually, because all nodes will spread to the next peripheral
 518 rectangular ring when the rescue tasks in the central area are completed. The dispersion of nodes

519 leads to the increase of distance between nodes; therefore, it takes longer for relay nodes to find the
 520 appropriate next hop nodes as the decreasing numbers of candidate next hop nodes. The
 521 distribution of mobile nodes is more uniform under the proposed FQMMBP, which shortens the
 522 delay.

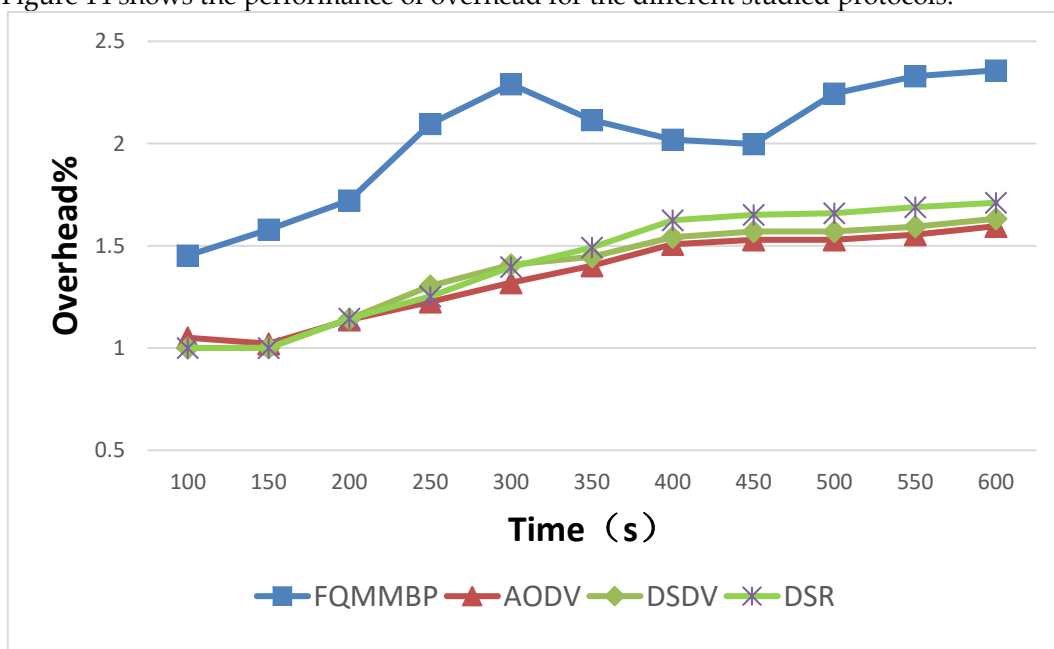


523 **Figure 13.** Comparison of delay for four protocols

524
 525 In the period of 200s to 300s, the delay increases obviously as the nodes spread to the next area
 526 around when they finish the rescue tasks in the central area. The node distribution changes from the
 527 original rectangular centralized to the rectangular ring decentralized, so the node distribution
 528 density becomes low, which increases the delay. After 300s, the delay tends to be stable. This is
 529 because there is no significant change in the distributions of nodes when they move from the area
 530 with $RUD=2$ to the areas with $RUD>2$. In that case, the delay tends to be stable because of the little
 531 impact on FQMMBP.

532 5.2.3. Overhead

533 Figure 14 shows the performance of overhead for the different studied protocols.



534 **Figure 14.** Comparison of overhead for four protocols

536 In terms of overhead, FQMMBP is significantly larger than other classical routing protocols.
537 That is because four new fields (*RUD*, *QL*, *QID* and *QW*) are added to RREQ message. Furthermore,
538 the dispersion of nodes increases the number of forwarding packets, which also contributes to the
539 increase of overhead. The data transmission overhead of AODV, DSDV and DSR protocols
540 increases with time, while FQMMBP meets the same rule from 100s to 300s. However, the overhead
541 of FQMMBP is decreasing between 300s and 450s, that is because before 300s, the rescue nodes are
542 distributed centrally, and they are far away from the destination nodes. Most of the data
543 transmissions rely on fixed relay nodes for forwarding, so the overhead is increasing. In the period
544 of 300s to 450s, the distribution of rescue nodes is scattered, and the average distance between
545 rescue nodes and destination nodes is close. In that case, the number of data forwarding is reduced,
546 so the overhead is reduced. After 450s, the distribution of rescue nodes is more scattered than
547 before, and the data communication between nodes relies on multi-hop forwarding, which makes
548 the data transmission overhead increasing. After 600 seconds, the overhead of FQMMBP can be
549 controlled within 2.5%. Although the performance of FQMMBP in overhead is not as good as the
550 other three protocols, it is worthwhile for the emergency rescue.

551 6. Conclusions

552 Protocols for post-earthquake emergency communication network are different with
553 traditional ones because of the heterogeneity and dynamicity of the network. After the earthquake,
554 Rescue urgency degree is related to in affected areas. In this paper, we first divide the whole
555 disaster area into several regions with different *RUD* values according to catastrophic intensity. A
556 four-quadrant mobility model for rescuers based on *RUD* is proposed. Under this mobility model,
557 we propose the FQMMBP protocol for emergency communication network, which improved the
558 RREQ message by adding four new fields: *RUD*, *QL*, *QID* and *QW*. Simulation results show that
559 FQMMBP is superior to traditional routing protocols (AODV, DSDV and DSR) in performances of
560 PDR and Delay. Although FQMMBP performs not as good as the other three protocols in
561 performance of overhead, it is worthwhile for the emergency rescue.

562 List of Abbreviations

563 ECN- Emergency communication network.
564 FQMM- Four-quadrant mobility model.
565 FQMMBP- FQMM-based protocol.
566 AODV- Ad hoc On-Demand Distance Vector Routing.
567 DSDV- Destination-Sequenced Distance-Vector Routing.
568 DSR- Dynamic Source Routing.
569 PDR- Package delivery rate.
570 DCHS- Deterministic cluster head selection.
571 RUD- Rescue urgency degree, which is inversely proportional to the seismic intensity value in this
572 area. The closer the area is to the epicenter, the lower the value of RUD is, which means the disaster
573 is serious and the priority of rescue is high; Otherwise, the opposite. When $RUD = 1$, the epicenter
574 disaster area is a rectangle; When $RUD > 1$, the disaster areas are rectangle rings that expands
575 outwards in turn.
576 ECV- Emergency communication vehicle.
577 BS- Base station.
578 UAV- Unmanned Aerial Vehicle.
579 PIE- Portable individual equipment.
580 QL- Quadrant Level, which is the number of times the quadrant divided.
581 QID- Quadrant ID.
582 RT- Number of Rescue Tasks.
583 NRA- Number of Rescuers Allocated.
584 GPS- Global Positioning System.
585 RREQ- Routing request.

586 **Competing interests**

587 The authors declare that they have no competing interests.

588 **Author's contributions**

589 All authors contribute equally.

590 **Acknowledgements**

591 This research was funded by Science and Technology Commission of Shanghai Municipality under Grant No.
592 18DZ1200500.

593 **Author details**

594 ¹Shanghai Earthquake Administration, No.87 Lanxi Rd, Shanghai, China.

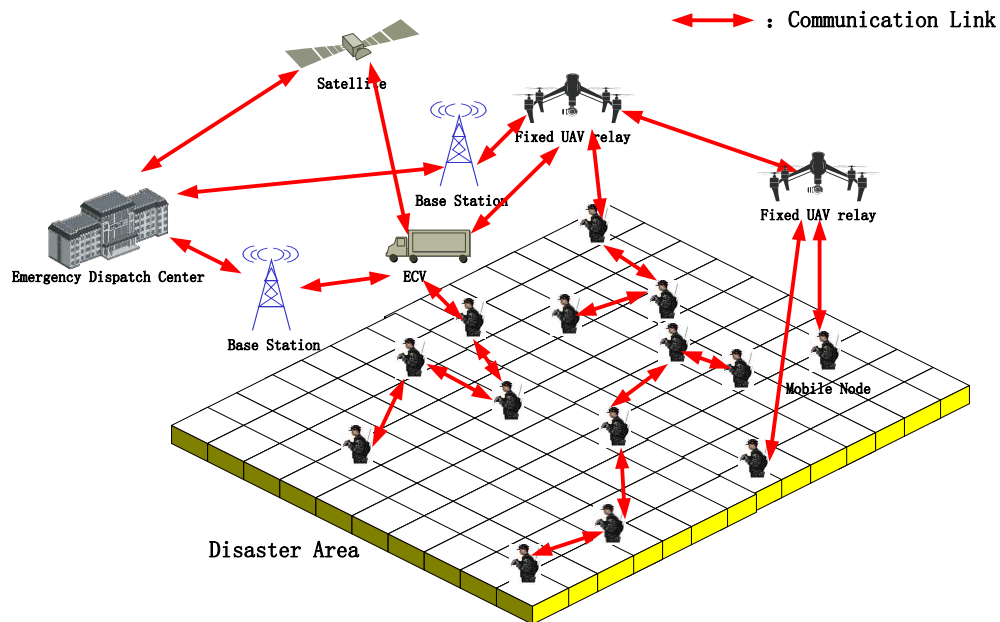
595 ²The College of Information, Mechanical, and Electrical Engineering, Shanghai Normal University, No. 100
596 Guilin Rd, Shanghai, China.

597 **References**

- 598 1. Hu Yuxian. *Earthquake engineering*, 2rd ed.; Seismological Press: Beijing, China, 2006; pp. 44–47, doi:
599 7502828524.
- 600 2. Wang Decai; Ni Sidao; Li Jun. Research Status of Rapid Assessment on Seismic Intensity. *Progress in*
601 *Geophysics* **2013**, *28*(4), 1772-1784, doi: 10.6038/pg20130418.
- 602 3. Hu Xinbu; He Zhengwen; Xu Yu. Robust Scheduling Optimization of Emergency Rescue Based on
603 Resource Constraints. *Operations Research and Management Science* **2013**, (2), 72-79, doi:
604 10.3969/j.issn.1007-3221.2013.02.011.
- 605 4. Yang Li; Liu Chengcheng; Song Li; et, al. Evaluation of Coal Mine Emergency Rescue Capability Based on
606 Entropy Weight Method. *China Soft Science* **2013**, (11), 185-192, doi: 10.3969/j.issn.1002-9753.2013.11.020.
- 607 5. Yuan Yuan; Fan Zhiping; Liu Yang. Study on the Model for the Assignment of Rescue Workers in
608 Emergency Rescue. *Chinese Journal of Management Science* **2013**, *21*(2), 152-160.
- 609 6. Song Ye; Song Yinghua; Liu Dan; et, al. Earthquake emergency rescue team's assignment model based on
610 time satisfaction and competence. *China Safety Science Journal* **2018**, *28*(8), 180-185, doi:
611 10.16265/j.cnki.issn1003-3033.2018.08.030.
- 612 7. Pan Xinchao; Liu Qinming; Ye Chunming. Capacity-Constrained Emergency Rescue After Earthquake
613 Disaster. *Journal of University of Shanghai for Science and Technology* **2017**, *39*(6), 549-555, doi:
614 10.13255/j.cnki.jusst.2017.06.008.
- 615 8. Li Mingyang; Qu Xiaoning; Li Bo; et, al. Model for Emergency Rescuers Assignment Considering Multiple
616 Disaster Areas. *Operations Research and Management Science* **2018**, *27*(8), 50-56, doi: 10.12005/orms.2018.0180.
- 617 9. Li Jin; Zhang Jianghua; Zhu Daoli. Multi-resource emergency scheduling model and algorithm in disaster
618 chain. *SYSTEMS ENGINEERING – THEORY & PRACTICE* **2011**, *31*(3), 488-495.
- 619 10. Cao Qingkui; Wang Wenjun; Ren Xiangyang. Emergency Rescue Workers Assignment Model
620 Considering Perception Satisfaction. *Value Engineering* **2017**, *36*(2), 82-85.
- 621 11. Li Mufeng; Tian Yu; Xu Hongfei; et, al. Research on Routing Algorithm of Wireless Sensor Network based
622 on Link Quality. *Netinfo Security* **2014**, (5), 59-62, doi: 10.3969/j.issn.1671-1122.2014.05.012.
- 623 12. Xue Lisi; Zhang Jie; Du Jiang. Research on DTN-based Routing Protocol of Earthquake Emergency
624 Communication. *Computer Technology and Development* **2017**, *27*(2), 182-186, doi:
625 10.3969/j.issn.1673-629X.2017.02.042.
- 626 13. Yu Xiang; Tu Siyu; Xu Xin. The Adaptive Routing Algorithm Based on Emergency Communications of
627 TD-LTE. *wuxian hulian keji* **2015**, (21), 1-4, doi: 10.3969/j.issn.1672-6944.2015.21.001.
- 628 14. Wang Xiaoming; Lin Yaguang; Zhang Shanshan; et, al. A social activity and physical contact-based
629 routing algorithm in mobile opportunistic networks for emergency response to sudden disasters.
630 *Enterprise Information Systems* **2017**, *11*(5), 597-626, doi: 10.1080/17517575.2015.1067840.
- 631 15. Ramalakshmi R, Radhakrishnan S. Weighted dominating set based routing for ad hoc communications in
632 emergency and rescue scenarios. *Wireless Networks* **2015**, *21*(2): 499-512, doi: 10.1007/s11276-014-0800-4.

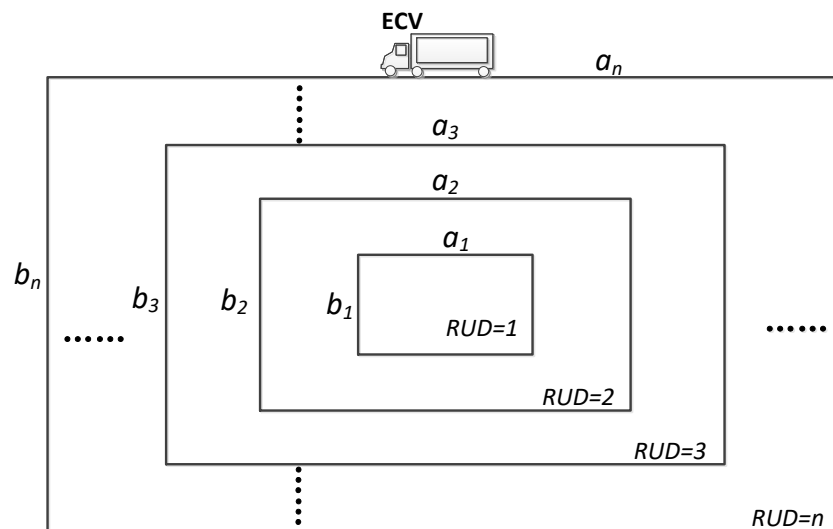
- 633 16. Arbia, D. B., Alam, M. M., Attia, R., & Hamida, E. B. A novel multi-hop body-to-body routing protocol for
634 disaster and emergency networks. In *2016 International Conference on Wireless Networks and Mobile*
635 *Communications (WINCOM)*, 2016: 246-252, doi: 10.1109/WINCOM.2016.7777222.
- 636 17. Bondre V, Dorle S. Performance Analysis of AOMDV and AODV Routing Protocol for Emergency
637 Services in VANET. *European Journal of Advances in Engineering and Technology* **2017**, 4(4): 242-248.
- 638 18. Ramakrishnan B, Nishanth R B, Joe M M, Selvi M. Cluster based emergency message broadcasting
639 technique for vehicular ad hoc network. *Wireless Networks* **2017**, 23(1): 233-248, doi:
640 10.1007/s11276-015-1134-6.
- 641 19. Camp T, Boleng J, Davies V. A survey of mobility models for ad hoc network research. *Wireless*
642 *communications and mobile computing* **2002**, 2(5): 483-502, doi: 10.1002/wcm.72.
- 643 20. Wang X, Li D, Zhang X, & Cao Y. MCDM-ECP: Multi Criteria Decision Making Method for Emergency
644 Communication Protocol in Disaster Area Wireless Network. *Applied Sciences* **2018**, 8(7): 1165, doi:
645 10.3390/app8071165.
- 646

647 **Figures**



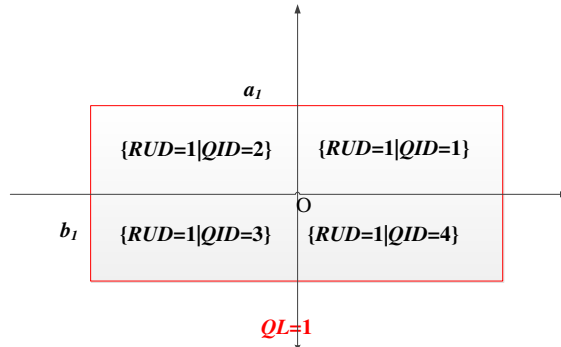
648
649

Figure 1. An example of post-earthquake ECN



650
651

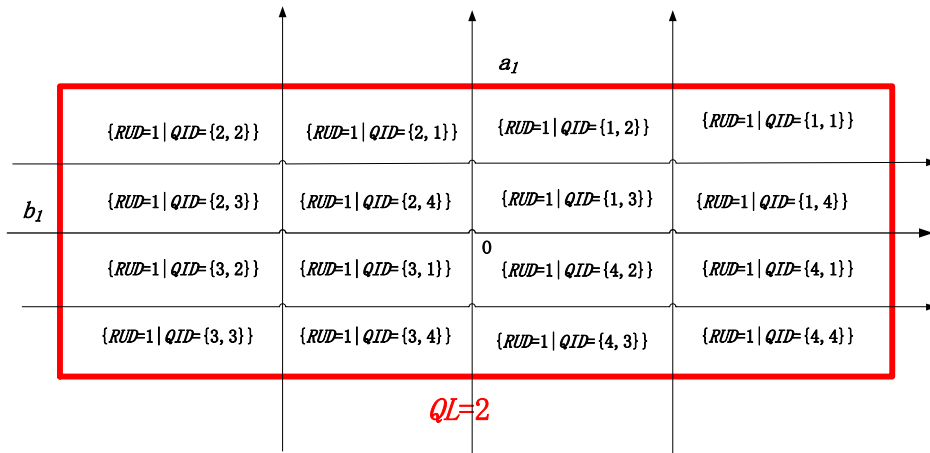
Figure 2. Disaster area division according to RUD



652

653

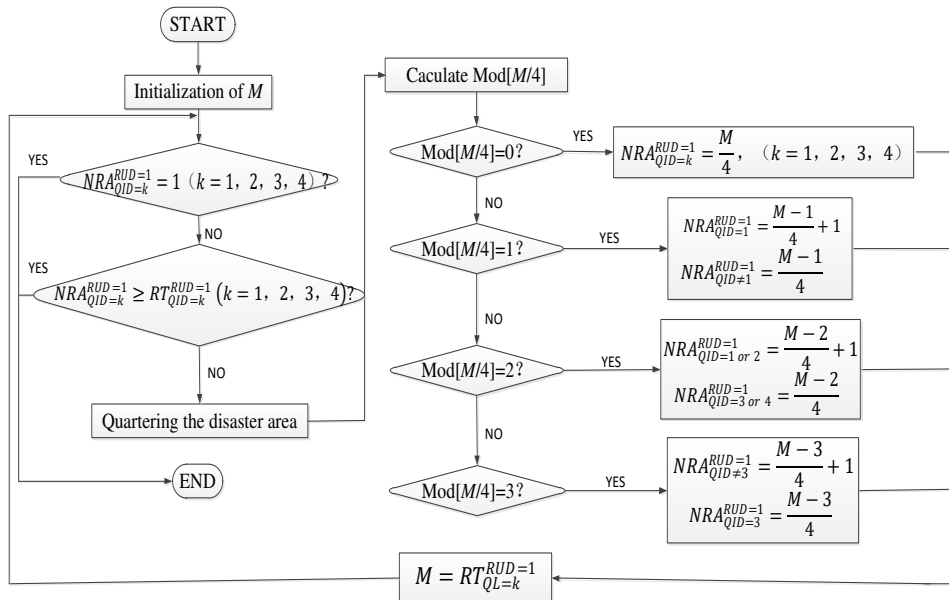
Figure 3. Disaster area with $RUD=1$ is divided into 4 quadrants for the first time ($QL=1$)



654

655

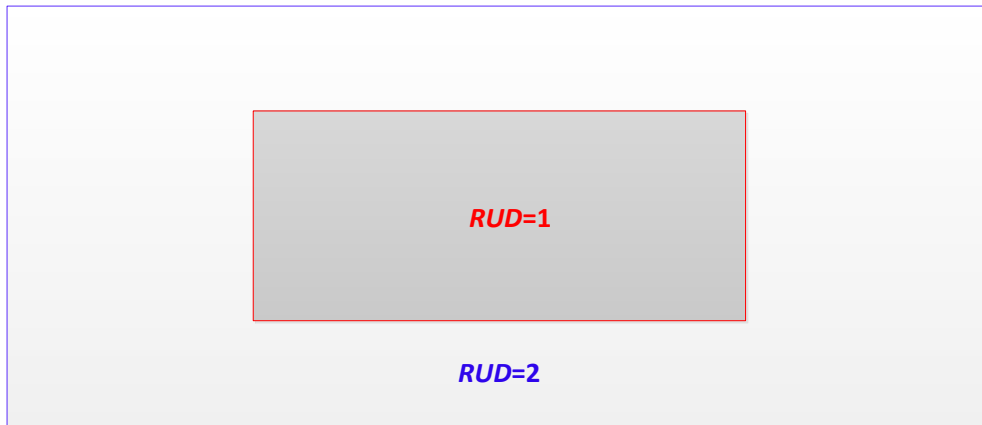
Figure 4. Disaster area with $RUD=1$ is divided into 16 quadrants for the second time ($QL=2$)



656

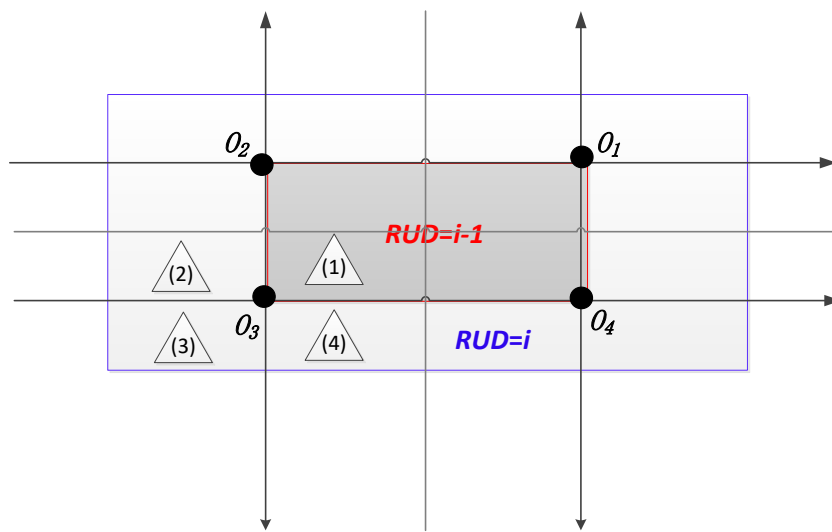
657

Figure 5. Allocation process of rescue nodes in disaster area with $RUD=1$



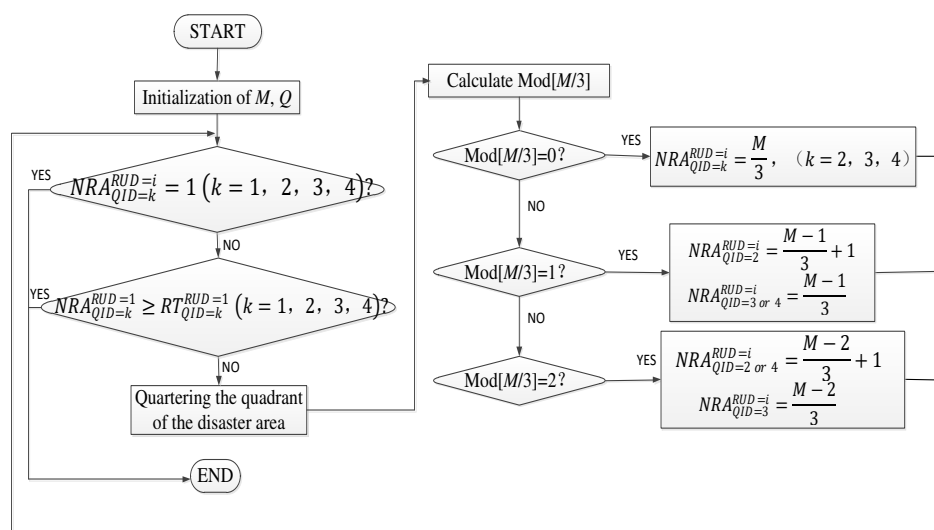
658
659

Figure 6. Rectangular ring with $RUD > 1$



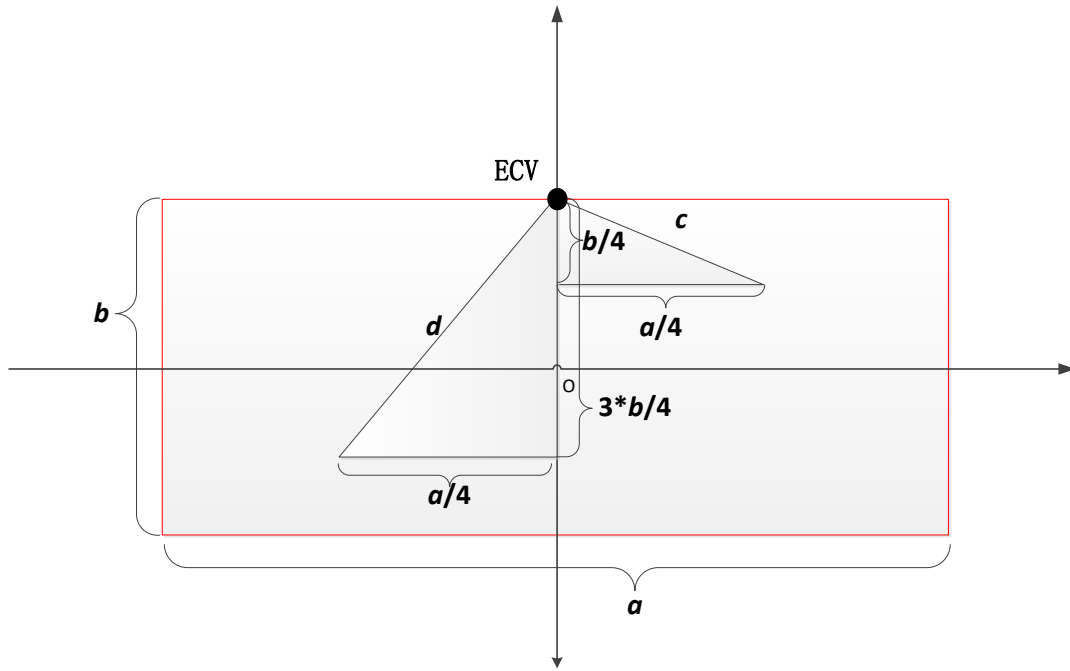
660
661

Figure 7. Disaster area with $RUD > 1$ is divided into 12 quadrants for the first time ($QL=1$)



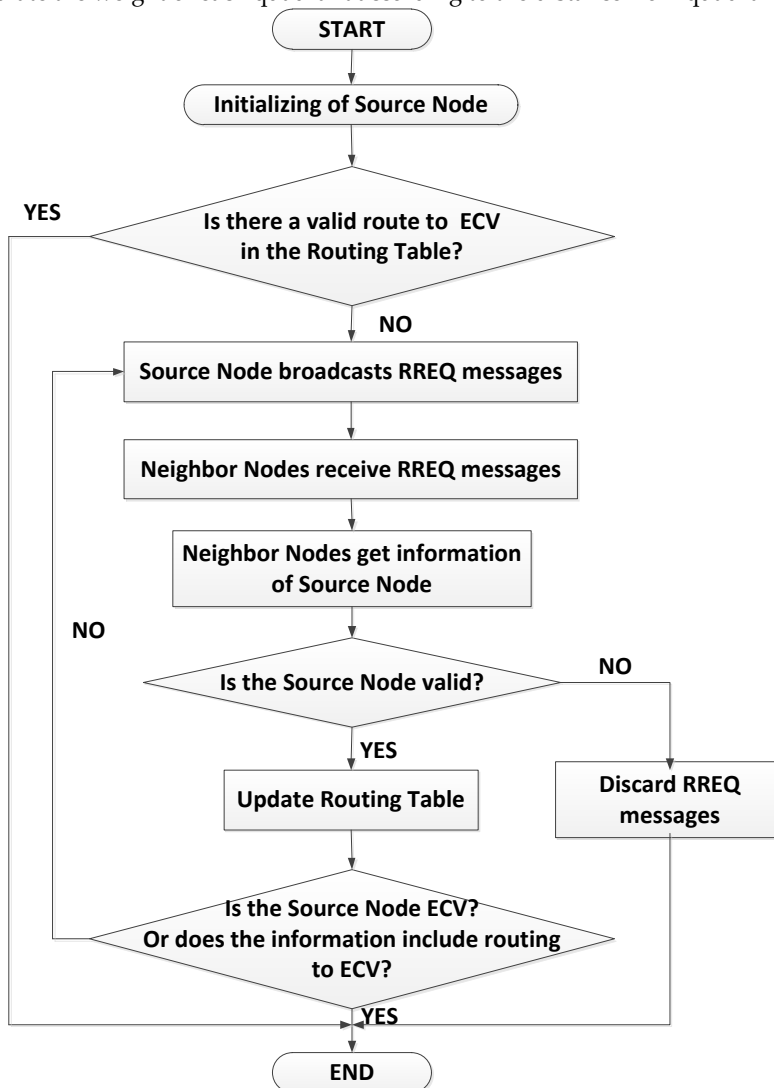
662
663

Figure 8. Allocation process of rescue nodes in disaster area with $RUD > 1$



664
665

Figure 9. Calculate the weight of each quadrant according to the distance from quadrant center to ECV



666
667

Figure 10. Routing establishment process for FQMMBP

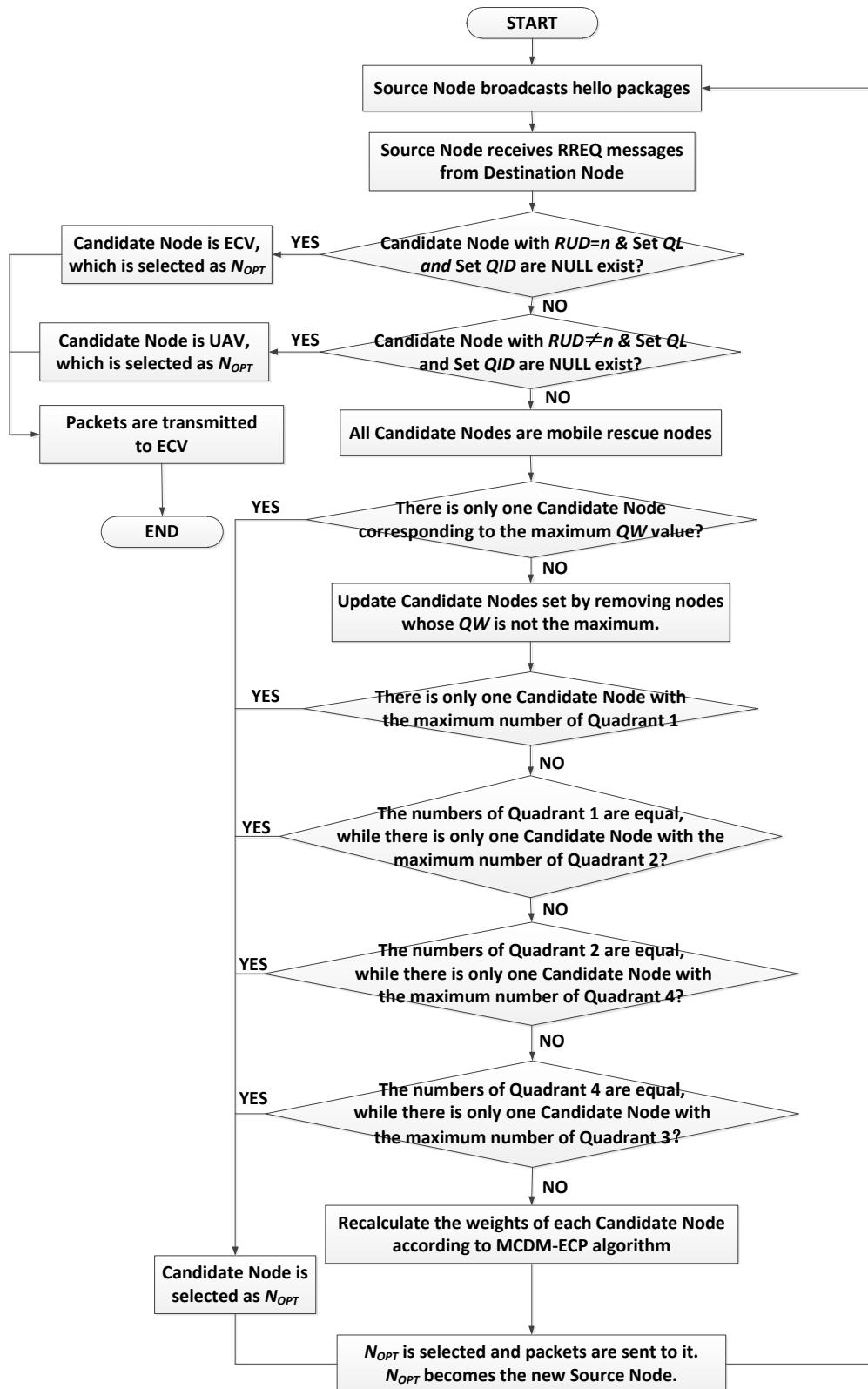
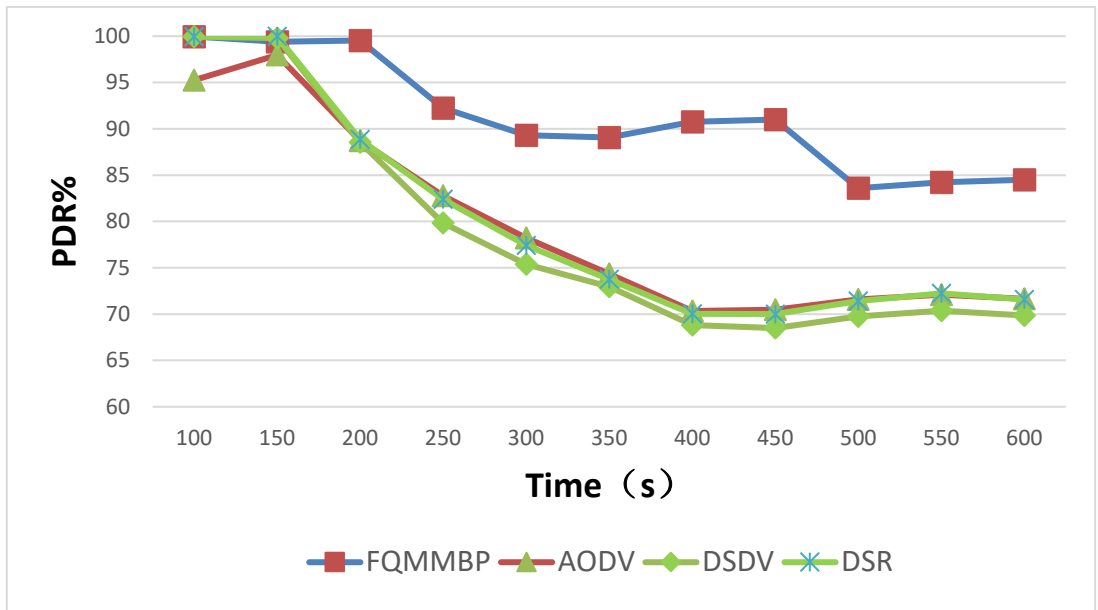
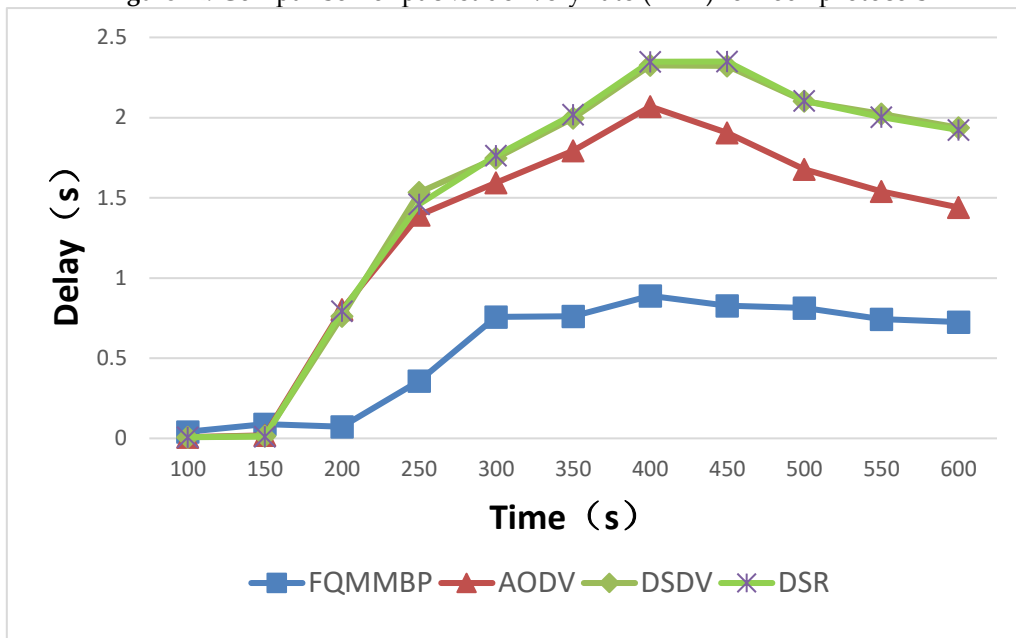


Figure 11. Routing maintenance process for FQMMBP



670
671

Figure 12. Comparison of packet delivery rate (PDR) for four protocols



672
673

Figure 13. Comparison of delay for four protocols

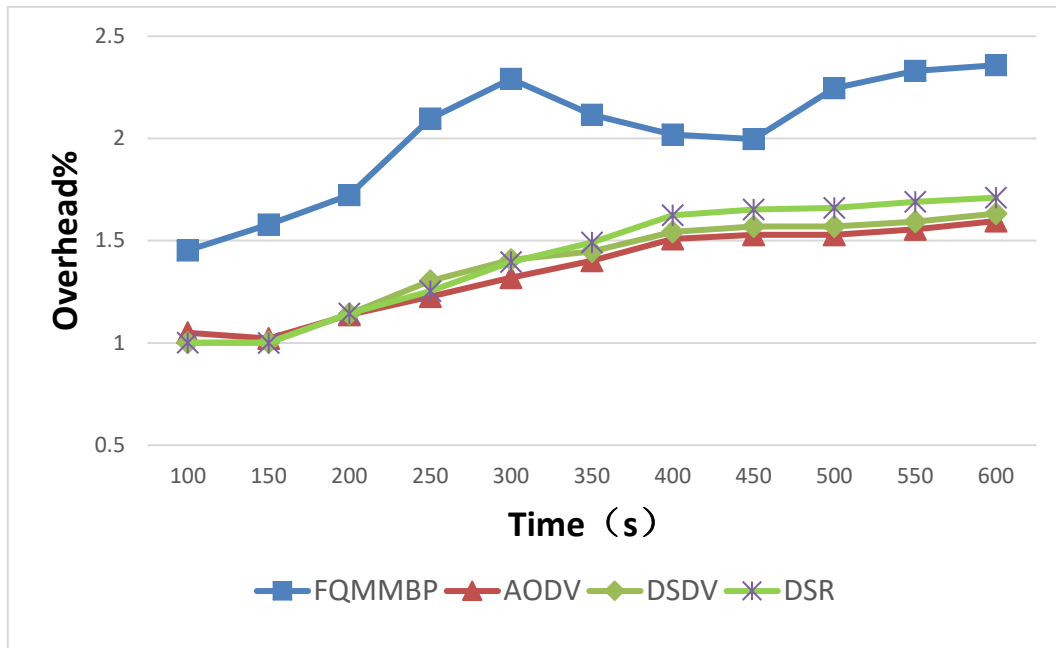


Figure 14. Comparison of overhead for four protocols

674
675

676
677
678
679
680

681 **Tables**

682

Table 1. Parameter definition and description

Parameters	Description
<i>RUD</i>	Rescue Urgency Degree, which is inversely proportional to the seismic intensity value in this area. The closer the area is to the epicenter, the lower the value of <i>RUD</i> is, which means the disaster is serious and the priority of rescue is high; Otherwise, the opposite. When <i>RUD</i> = 1, the epicenter disaster area is a rectangle; When <i>RUD</i> > 1, the disaster areas are rectangle rings that expands outwards in turn.
<i>a_i</i>	Length of area where <i>RUD</i> = <i>i</i> .
<i>b_i</i>	Width of area where <i>RUD</i> = <i>i</i> .
<i>QL</i>	Quadrant Level, which is the number of times the quadrant divided.
<i>QID</i>	Quadrant ID.
<i>RT</i>	Number of Rescue Tasks.
<i>NRA</i>	Number of Rescuers Allocated.
<i>M</i>	Number of mobile nodes.

683

684

Table 2. The improved RREQ data format.

Type	Flags					Reserved	Hop Count
	J	R	G	D	U		

RREQ ID

Destination IP Address

Destination Sequence Number

Source IP Address

Source Sequence Number

RUD

QL

QID

QW

685

686

Table 3. Simulation Parameters.

Parameters	Values
Number of mobile rescue nodes (<i>M</i>)	48
Fixed communication nodes (ECV included)	3
Simulation time span	600s
Area of earthquake affected regions	10km*10km
<i>a</i> ₁	6km
<i>b</i> ₁	4km

687

Figures

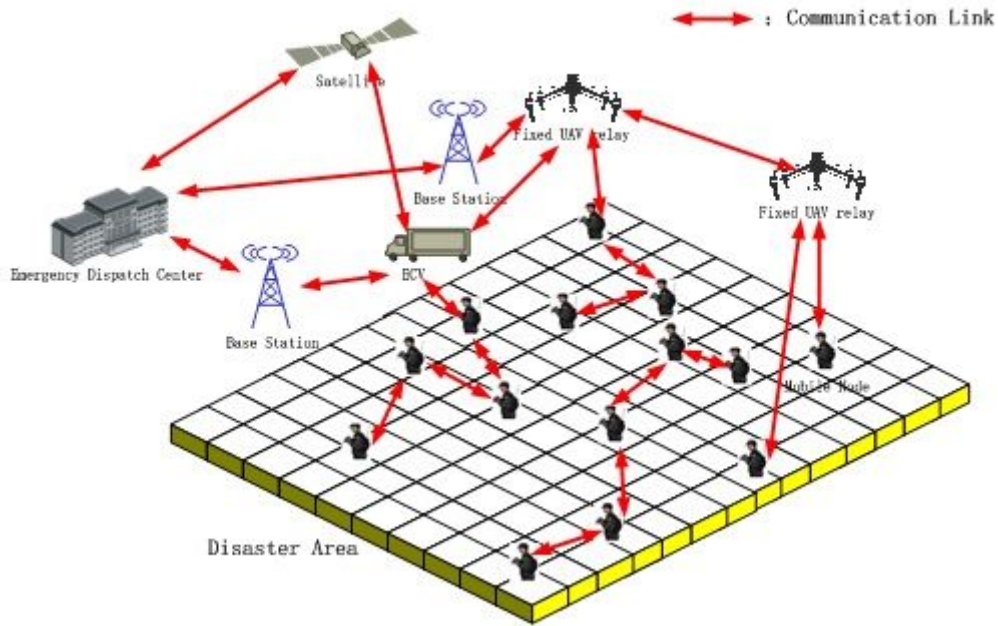


Figure 1

An example of post-earthquake ECN

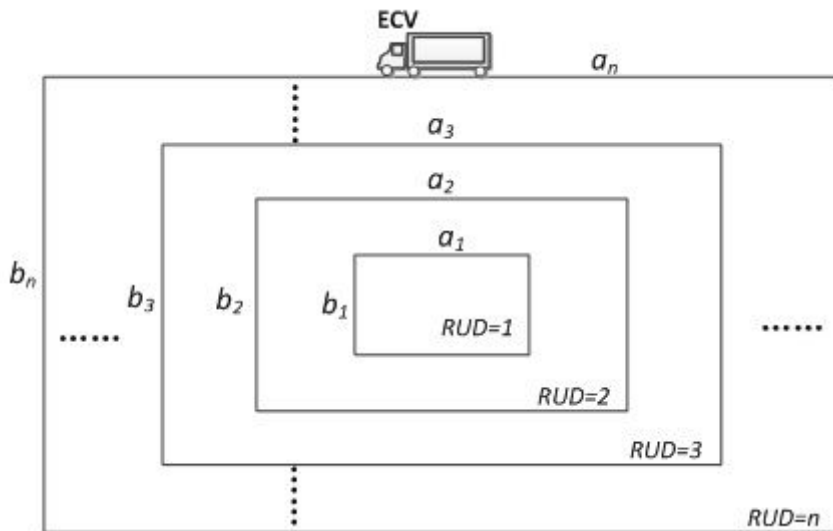


Figure 2

Disaster area division according to RUD

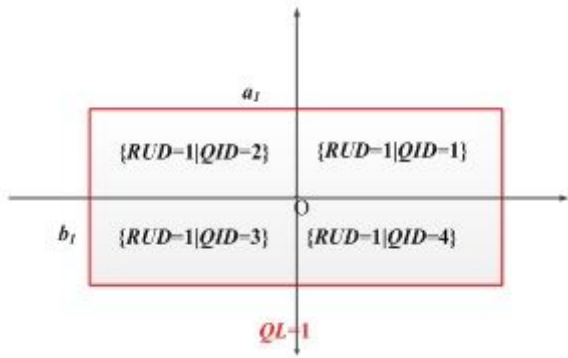


Figure 3

Disaster area with RUD=1 is divided into 4 quadrants for the first time (QL=1)

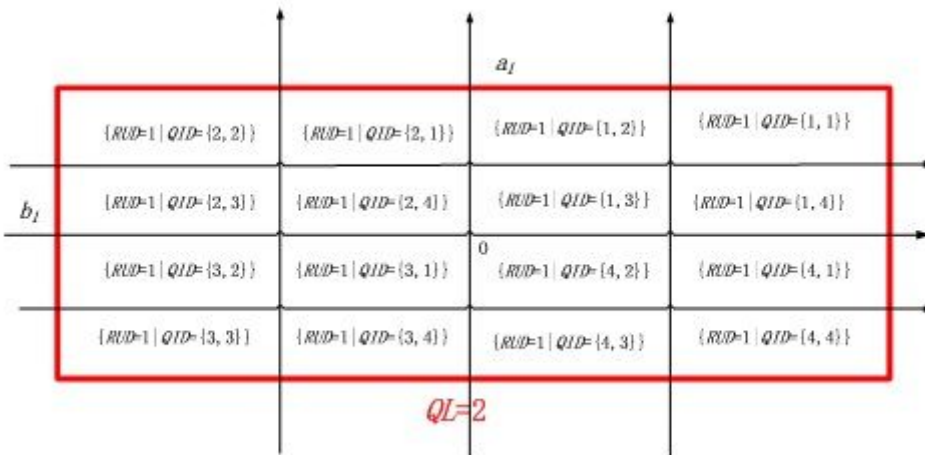


Figure 4

Disaster area with RUD=1 is divided into 16 quadrants for the second time (QL=2)

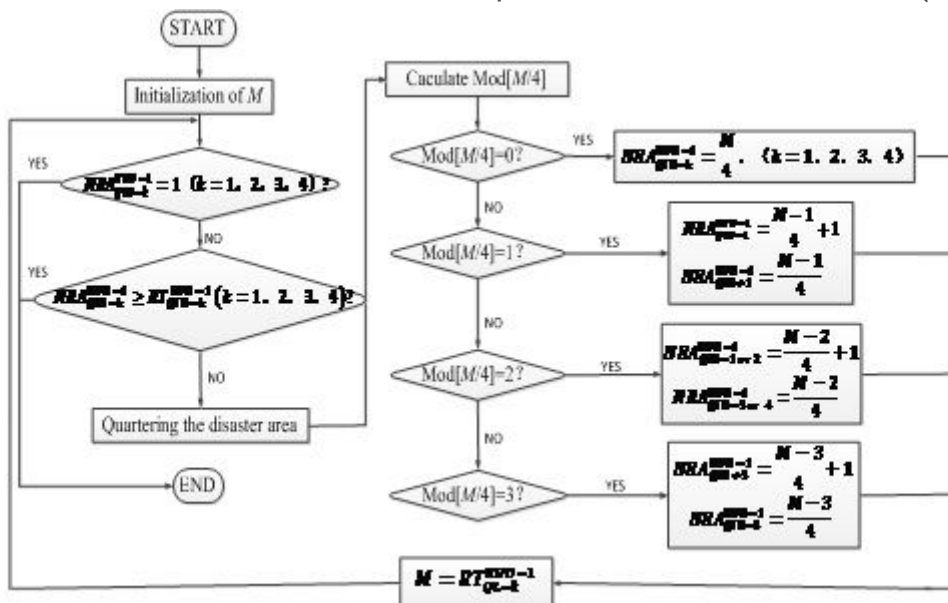


Figure 5

Allocation process of rescue nodes in disaster area with $RUD=1$



Figure 6

Rectangular ring with $RUD > 1$

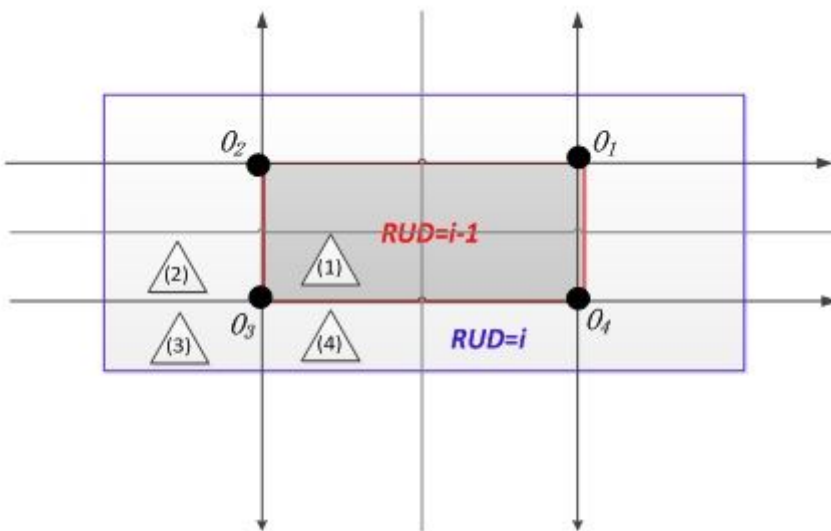


Figure 7

Disaster area with $RUD > 1$ is divided into 12 quadrants for the first time ($QL=1$)

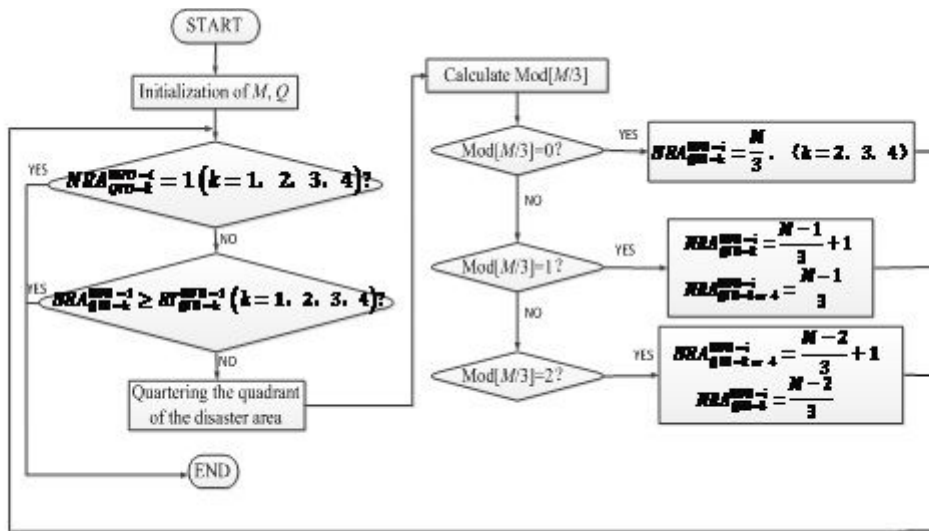


Figure 8

Allocation process of rescue nodes in disaster area with $RUD > 1$

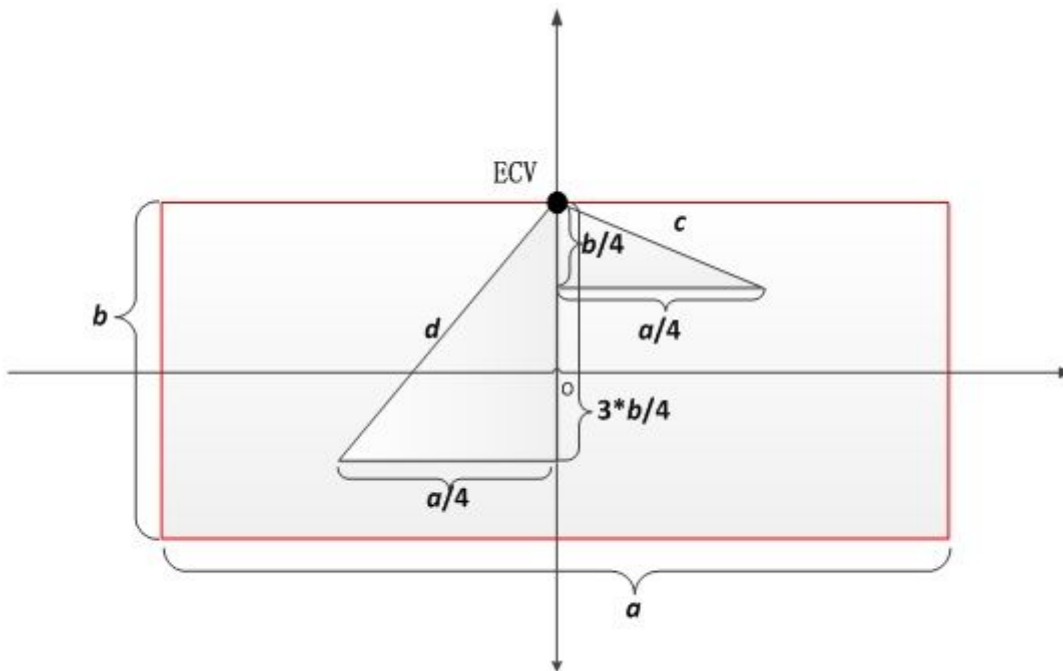


Figure 9

Calculate the weight of each quadrant according to the distance from quadrant center to ECV

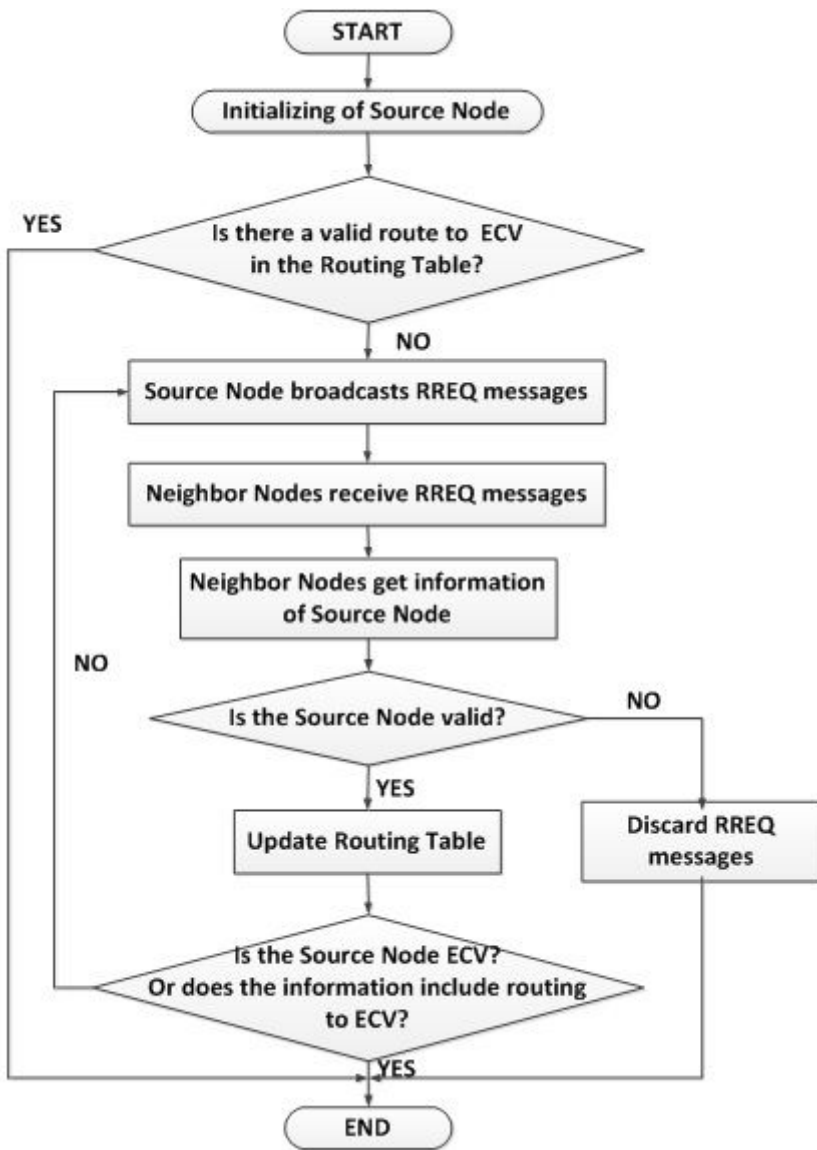


Figure 10

Routing establishment process for FQMMBP

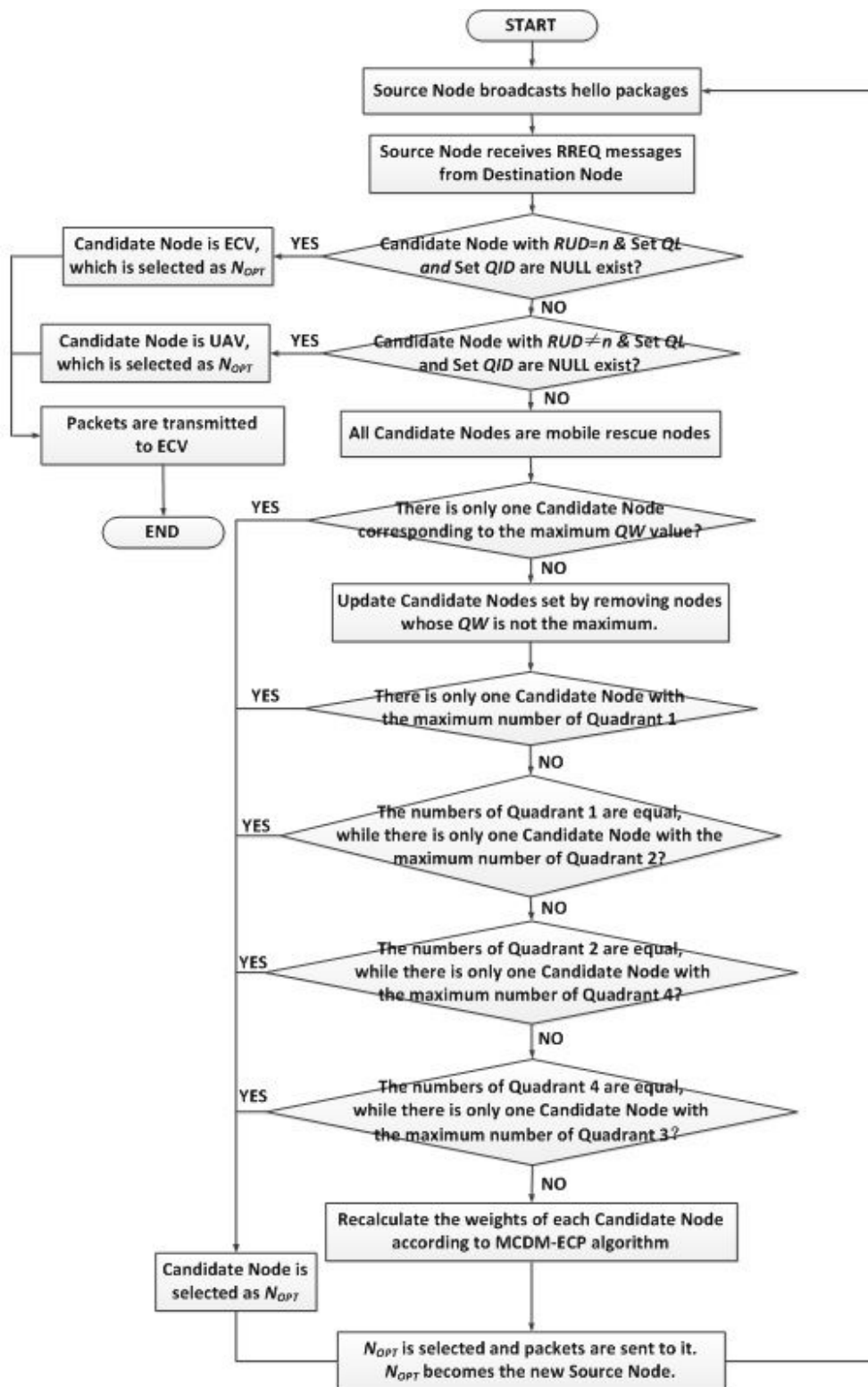


Figure 11

Routing maintenance process for FQMMBP

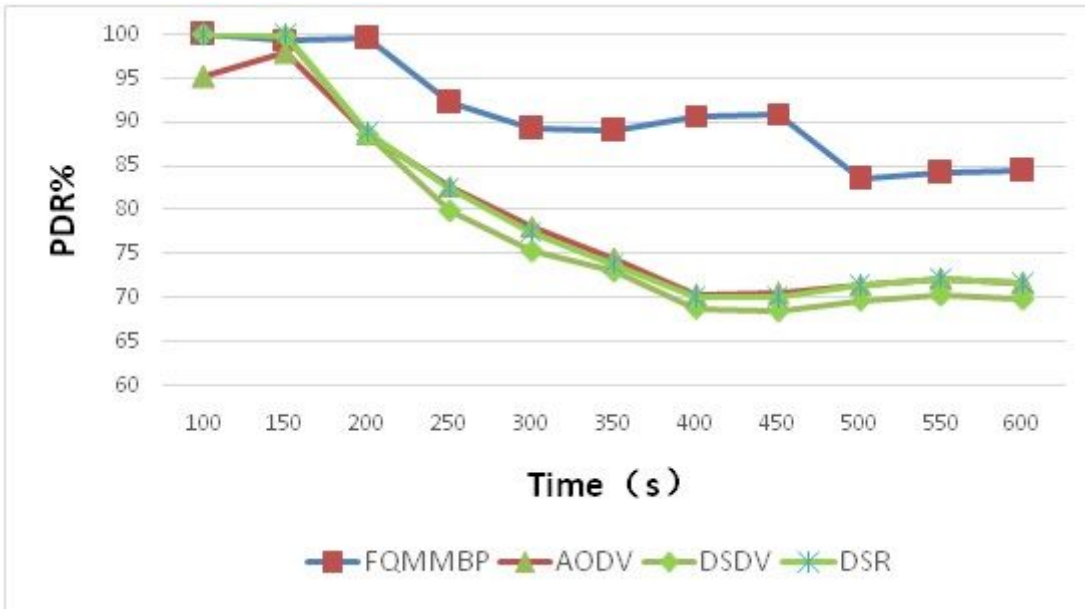


Figure 12

Comparison of packet delivery rate (PDR)for four protocols

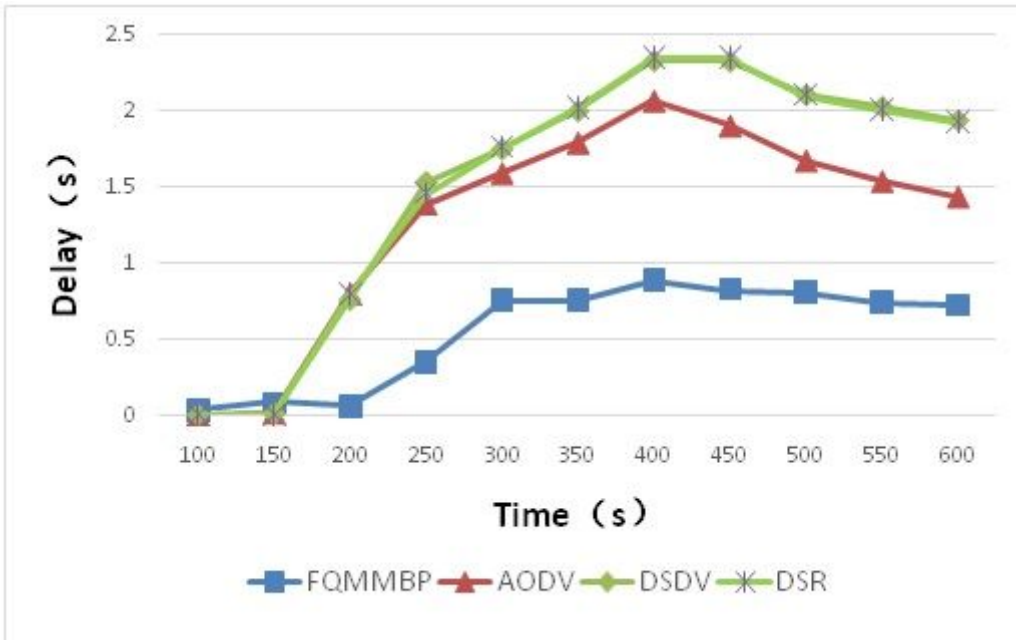


Figure 13

Comparison of delay for four protocols

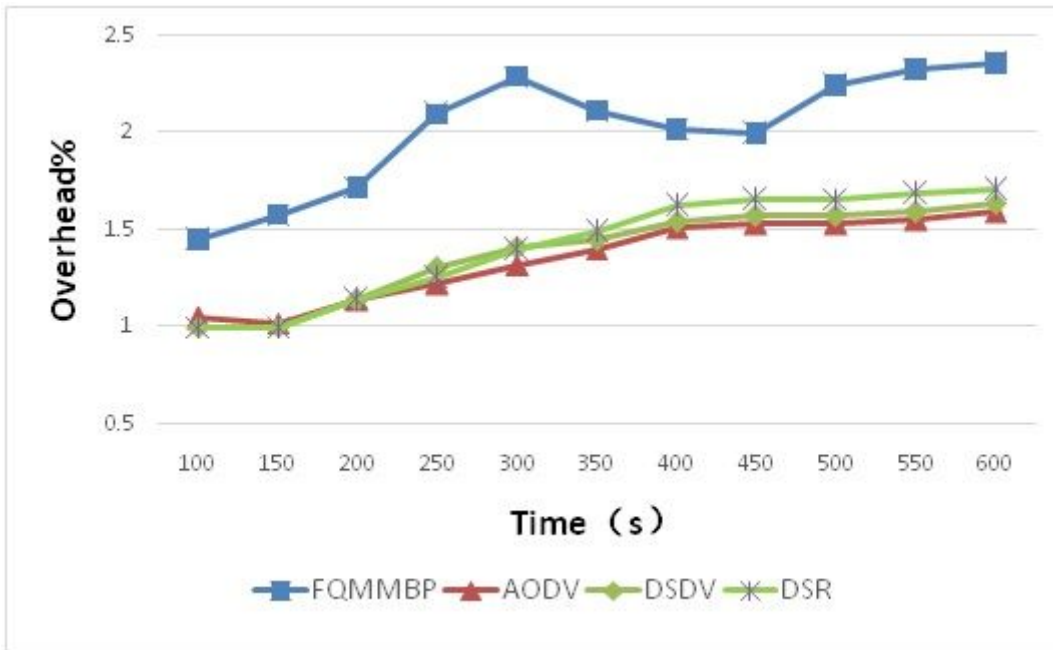


Figure 14

Comparison of overhead for four protocols

Supplementary Files

This is a list of supplementary files associated with this preprint. Click to download.

- [authorbiography.pdf](#)
- [authorPhotograph.jpg](#)